ASSESSING REINFORCED CONCRETE BEAM CAPACITY: FINITE ELEMENT ANALYSIS AND VALIDATION

A Thesis submitted in partial fulfillment of the requirements for the award of a degree of
Bachelor of Science in Civil Engineering
by

Ahmed Mohamed Omar
(ID: 193-47-1106)

Supervised by

Md. Mehedi Hassan Bhuiyan
Lecturer

Department of Civil Engineering
Daffodil International University

Department of Civil Engineering

Faculty of Engineering

DAFFODIL INTERNATIONAL UNIVERSITY

12th - February – 2024

CERTIFICATION

This certifies that the student shown below completed the project and thesis titled "**Assessing Reinforced Concrete Beam Capacity: Finite Element Analysis and Validation**" under my supervision. The investigation has been carried out at the labs of the Department of Civil Engineering, Faculty of Engineering, Daffodil International University, as part of the requirements for the Bachelor of Science in Civil Engineering degree. The presentation of the work was successfully held on 12 February 2024.

Signature of the candidate

18/2/2024

Name: Ahmed Mohamed Omar

ID: 193-47-1106

Countersigned

18.02.2024

Md. Mehedi Hassan Bhuiyan

Lecturer

Department of Civil Engineering

Faculty of Engineering

Daffodil International University.

The project and thesis titled **" Assessing Reinforced Concrete Beam Capacity: Finite Element Analysis and Validation,** "submitted by Ahmed Mohamed Omar, ID No: 193-47-1106, Session: Fall 2019, has been accepted as satisfactory. This work fulfils, in part, the requirements for the Bachelor of Science in Civil Engineering degree. Date of Acceptance: 12 February 2024

BOARD OF EXAMINERS

Md. Mehdi Hassan Bhuiyan — Supervisor
Lecturer
Department of CE, DIU

Dr. Mohammad Hannan Mahmud Khan — Chairman
Assistant Professor & Head Department of CE
Department of CE, DIU

Dr. Miah M. Hussainuzzaman — Internal Member
Associate Professor
Department of CE, DIU

Mr. Md. Masud Alom — Internal Member
Assistant Professor
Department of CE, DIU

Md. Rasel Chowdhury — External Member
Deputy Director
Padma Associates and Engineers Limited

DEDICATION

I dedicated my thesis to my beloved parents, whose steadfast support and generosity have been the cornerstone of my academic journey. Your support and confidence in my skills have been the primary motivation behind my actions.

I want to convey my sincere appreciation to my dear Father. Your unwavering assistance, motivation, and confidence have been the bedrock of my progress. The sacrifices and insights you have imparted to me have profoundly influenced my identity. This achievement is equally attributable to both you and me. I appreciate your role as my beacon of guidance.

I am grateful to my family, whose love, compassion, and patience have given me unwavering support. The unwavering support and confidence you have always shown in my aspirations have motivated me to achieve tremendous success.

I sincerely appreciate my educators and mentors, whose counsel and sagacity have influenced my scholarly studies. Your commitment to developing knowledge and promoting intellectual curiosity has been highly beneficial.

This work is devoted to those who have played a vital part in my life, actively contributing to my personal development and achievements. I appreciate your unwavering role as my perpetual wellspring of motivation and assistance.

CONTENT

TABLE OF CONTENT

LIST OF FIGURES

LIST OF TABLES

LIST OF ABBREVIATION

fc'	Compressive strength of concrete
fy	Yield strength of steel
E_s	Modulus of Elasticity
ε_y	Strain
ψ	Dilation angle

ACKNOWLEDGEMENT

I begin by thanking Allah or God, the source of all knowledge and power, for giving me the perseverance and resilience required to finish this project.

I want to express my genuine gratitude to **Md. Mehedi Hassan Bhuiyan, Lecturer** of the **Department of Civil Engineering**, for his guidance and support as my project and thesis supervisor. The individual's unwavering commitment, assistance, and direction have played a crucial role in the success of this activity. I express my gratitude for his invaluable counsel and support, which have greatly helped the successful completion of this thesis.

I also want to thank **Dr. Mohammad Hannan Mahmud Khan**, the **head of the Department of Civil Engineering and assistant professor**, for all his assistance, encouragement, and support.

I want to express my heartfelt gratitude to **Yusuf Abdirahman Nor** for his outstanding support in supplying me with an extra laptop. This assistance greatly expedited the completion of my thesis project. The individual's benevolence and will to assist have been crucial to my educational path.

We extend our heartfelt gratitude and affection to our treasured family and friends. Their unfailing support, inspiration, and encouragement have been indispensable throughout my educational journeys at this University.

Abstract

The experimental capacity for reinforced beams is validated in this study through finite-element analysis using ABAQUS. Both spliced and un-spliced configurations are taken into consideration in this investigation. Considering several modeling methodologies, such as the dilation angle, viscosity, and meshing parameters, the three beams, each sized 2000 × 250 × 150 mm, I verified the findings of a prior study report using Normal Strength Concrete as the material(Mabrouk & Mounir, 2018). I conducted several trials throughout the validation procedure to identify a final validation graph that closely resembles the graph plot in the previous study report. After examining viscosity, it was determined that the ideal values for B-1, B-2, and B-3 were 0.04, 0.05, and 0.025, respectively. A dilation angle of 31 degrees was consistently used throughout all beams, effectively producing successful results. Several different mesh sizes were investigated, and the results showed that a standard 25mm mesh size is suitable for all beams. In addition to enhancing the reliability of the findings of finite-element analysis, this systematic assessment guarantees that a thorough knowledge of the structural behavior of reinforced concrete beams is achieved. This evaluation also contributes significantly to structural engineering by providing valuable insights.

Keywords: Dilation angle, Viscosity, Mesh, finite element analysis, Normal Strength concrete, ABAQUS.

CHAPTER 1
INTRODUCTION

1.1 General

Normal Strength Concrete (NSC) is a standard concrete mixture with a compressive strength typically between 2,500 to 6,000 pounds per square inch (psi). It is widely employed in many construction endeavors. The primary function of this material is to provide compressive strength, while the steel reinforcement improves tensile strength and prevents brittle fracture. The design and study of NSC (Normal Strength Concrete) reinforced concrete beams consider material characteristics, load-carrying capacity, and cracking patterns. Finite Element analysis is employed to replicate the behavior of beams subjected to different loads, enabling the prediction of deflection and the occurrence of fracture forms. Verifying these simulations using empirical data aids in comprehending their structural efficacy.

Finite Element Analysis (FEA) is a reliable method used in structural engineering to make exact computer models of materials that make up structures. It has been shown to work well for showing and studying the nonlinear properties of reinforced concrete parts. The finite element method has come a long way since the 1970s, especially when analyzing reinforced concrete buildings. Concrete is a complicated substance whose qualities are affected by many things. It is hard to tell when concrete breaks down because the stress-strain relationship is not straight, and strain is hardening and softening. In structural engineering, it is essential to accurately evaluate reinforced concrete beams to ensure that structures are safe, strong, and fit together well.

This study aims to combine Finite Element Analysis (FEA), a widely recognized method for accurate numerical modeling, with constitutive material models and actual testing. This project aims to improve our understanding of the complex behavior of reinforced concrete beams by integrating theoretical models with practical experimental data. Its objective is to make significant contributions to the field of structural engineering.

1.2 Lap Splice

A lap splice in reinforced concrete beams overlays two lengths of reinforcing bars inside a specified portion of the beam. The act of overlapping, sometimes referred to as a lap splice length, is a critical method of detailing that aims to improve the structural strength and ability to bear loads of the beam. A demo Figure of a Lap Splice (Fig. 1.1: An illustrative representation of a Lap splice) is given below.

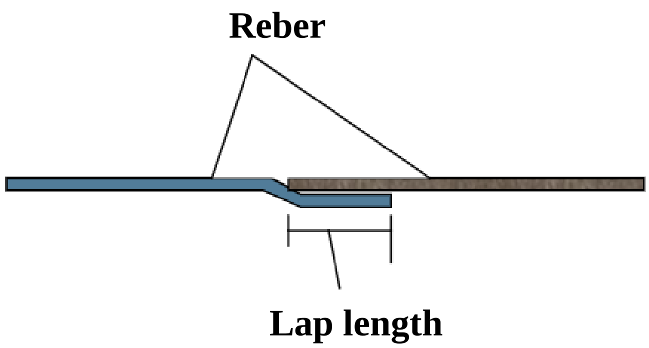

Fig. 1.1: An illustrative representation of a Lap splice

1.2.1 Benefits and Drawbacks of Lap Splice for Beams:

1.2.1.1 Benefits of Lap Splice for Beams:

1) Ensures smooth transmission of loads and maintains structural integrity.
2) Enhances the ability to withstand increased loads by strengthening the flexural capacity.
3) Improves the ability to deform without breaking, which is especially important in regions prone to earthquakes.
4) Enhances the overall structural efficiency.

1.2.1.2 Drawbacks of Lap Splice for Beams:

1) Possible reduction in shear strength; could need further reinforcing.
2) Construction obstacles need accurate positioning and alignment of bars.

1.2.2 Types of Splices

There are many types of lap splices, and each has different purposes according to the needs of the building. These are a few common categories:

i. **Simple Lap Splice:** The process of joining two sections of rebar by overlapping them to create a continuous reinforcement is known as Simple lap splicing. This allows the efficient distribution of loads over the whole structure. There are two kinds of lap splices: contact lap splices and non-contact lap splices. The overlapping portions of contact lap splices are interconnected using wires. Non-contact lap splices consist of lapped portions that do not come into direct contact with each other. These splices are allowed in practice as long as the distance between the lap sections matches the standards stipulated in the code.

ii. **Welded Splicing**: Welded splicing is a welding method used to connect reinforcing bars, allowing for the transmission of stresses through the weld. It is especially beneficial for rebars with a diameter more significant than 36mm. This technique establishes an effective and immediate connection between the intersecting extremities of reinforcing bars, ensuring the efficient transmission of forces and increasing the structural soundness of concrete components. This method is appropriate for scenarios involving the usage of thicker rebars, as it provides a practical and long-lasting bond between the bars.

iii. **Mechanical Splicing:** This splicing technique involves the mechanical connection of bars in direct contact using sleeves or similar devices. This method entails establishing connections between two rebar components, allowing them to operate at uninterrupted lengths. Mechanical splices connect rebar in a way that is similar to a continuous piece of rebar, providing several benefits. Mechanical splicing technologies are highly adaptable, making them ideal for use in densely packed reinforcement regions and construction joints at project sites. This method guarantees dependable connections between individual lengths of rebar, hence enhancing the overall strength and stability of the reinforced concrete building. A demo Figure of different types (Fig. 1.2) is given below.

Fig. 1.2: Different Types of Splicing

1.3 Stirrups

Stirrups are essential in reinforced concrete constructions, usually as closed loops or ties strategically positioned around vertical rebars. The main objective of these elements is to bolster the structural strength of concrete components, particularly in beams and columns, by resisting shear stresses, avoiding diagonal cracking, and providing lateral support to the longitudinal reinforcement. Stirrups are essential for enhancing the ability of a structure to deform without breaking and for improving its overall performance when subjected to different types of loads. Within the scope of the inquiry, a comprehensive analysis is conducted on four specific variations of stirrups: Vertical, Rectangular, Corrugated, and Spiral (Mabrouk & Mounir, 2018). Different Shapes of Transverse reinforcement or Stirrups are shown in the figure below (Fig. 1.3)

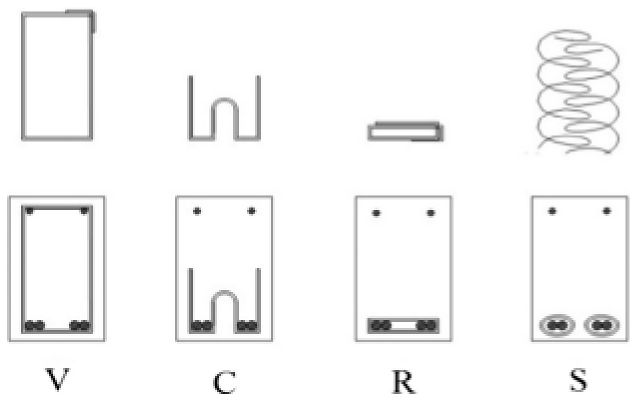

Fig. 1.3 Different shapes of transverse reinforcement

1.4 Scope of Study

The study applied finite element software to predict the deflection and fracture patterns in beams made of normal-strength concrete. A three-dimensional beam model is constructed to comprehend the behavior of the control beam. The experimental results are validated using Reinforced Concrete beams, which improve the comprehension of structural engineering by comparing failure parameters and proving the agreement between finite element analysis and empirical findings.

1.5 Objective

The main objective of this study is to validate the experimental capacity of reinforced beams, considering both beams with and without splices, using the finite-element package. The primary aim is to assess the effectiveness and accuracy of different modeling approaches, including modifying parameters such as dilation angle, viscosity, and meshing. The study aims to improve the reliability of finite element models in recreating the experimental performance of reinforced concrete beams and contribute knowledge in structural analysis via thorough computational or finite element validation.

1.6 Outline of thesis

Chapter 1. Provides an overview of the fundamental concept of the investigation.

Chapter 2. A literature study exploring previous research on failure parameters, FEA, and RC beams.

Chapter 3. The methodology employed for FEA simulations and analysis of failure parameters.

Chapter 4. After thoroughly verifying the FEA model, the assessment results are presented, and comparisons are made with experimental data.

Chapter 5. Summarises the main conclusions and lays out the recommendations generated from the research.

CHAPTER 2
LITERATURE REVIEW

2.1 Introduction

A literature review is an overview summary incorporating several academics' knowledge to comprehend a particular subject matter thoroughly. It is often used in articles and research papers to examine several perspectives on a specific subject. A literature review is a crucial tool for researchers to effectively traverse the extensive pool of information about a particular topic rather than existing as an isolated entity. It is the first reference for comprehensive investigations, offering a contemporary and helpful summary. Additionally, it assists in establishing the analytical framework for research papers, offering a robust basis for novel concepts. A literature review is a dynamic approach to engaging with the conceptual framework of a subject rather than only inquiring. It encourages engagement in scholarly discourse, assesses existing viewpoints, and adds to a versatile conversation on a particular subject. It is essential for most research initiatives since it improves the research process and enables a thorough and informed investigation.

2.2 Overview

This chapter summarises the author's future goals and highlights essential lessons learned from the literature study. The purpose of the discussion is to highlight the significance of the author's intended research in terms of advancing the area. The study's importance in expanding knowledge in the selected field should be evident to readers, who should also be aware of the author's growing comprehension.

2.3 Literature review

This section offers a detailed and comprehensive summary of the publications and research papers examined throughout the review process, providing a complete overview of the subject.

(Maghsoudi & Akbarzadeh Bengar, 2011) This study examined ABAQUS-analyzed continuously strengthened concrete (RC) beams reinforced with CFRP laminates. The research involves creating a 3D beam model with 250 × 150 × 6000 mm dimensions and including CFRP reinforcement features. The study investigates the influence of CFRP on the length of beam fractures and deflection, uncovering a restricted level of flexibility at 3. This discovery facilitates the development and reinforcement of concrete beams using CFRP laminates, enhancing comprehension in structural engineering. The experimental results demonstrated that CFRP-reinforced beams had denser cracking and tighter fracture gaps than control beams. The reinforced beams had three stages: pre-cracking concrete, post-cracking concrete with tension steel pre-yield, and post-yield tension steel behavior. Multiple CFRP layers affected the failure mechanism, reducing end separation but not intermediate crack debonding. The load-deflection graphs demonstrated that reinforced beams had higher stiffness after cracking and before yielding. More CFRP layers reduced beam stiffness loss following tensile steel yielding. Extra CFRP layers increased the steel's tensile and yield strengths under stress, improving load-bearing. In particular, adding one, two, or three CFRP sheets increased ultimate load capacity by 18%, 30.05, and 60%, respectively, compared to the control beam.

(Mousa, 2015) This study investigates the flexural performance of concrete beams with different tension-reinforcing lap splice lengths. This research explores the complex relationships between many structural components, including splice length, bar diameter, cross-sectional reinforcement, anchor form, and concrete cover. The study investigates two classifications of high-strength concrete, characterized by compressive strengths of 55 and 65 MPa, respectively. The first category lacks silica fume, whereas the second group consists of 10.05 silica fume. The tension reinforcement is created by joining two distorted bars at the area where the moment stays consistent. The study's results suggest that transverse reinforcement is essential for achieving adequate ductility responses. Including stirrups, particularly at splice ends and hooked end splices, improves flexibility due to increased cracking and ultimate loads. The study examines the relationships between the diameter of bars, the amount of concrete covering the bars, and the presence of silica fume in connection to the splicing of tension reinforcement in concrete beams.

(Demir et al., 2016) This work presents a numerical finite element model using ABAQUS software, which incorporates reliable modeling approaches and constitutive material models to simulate reinforced concrete deep beams precisely. The comparison between numerical and experimental findings demonstrates the efficacy of ABAQUS in accurately modeling yield, ultimate load levels, and damage distribution. The study's results indicate that a dilation angle of 56 degrees is suggested due to its strong positive impact on deep beams' ultimate load capacity and flexibility. The discrepancies in the finite element model following the first fracture may be attributed to the lack of micro-cracks and other external causes. Generally, this technique successfully evaluates the non-linear characteristics of reinforced concrete deep beams.

(Vitanov, 2017) The sensitivity of the dilation angle in numerical simulations of reinforced concrete (RC) deep beams is examined in this work using the ABAQUS program. Parametric nonlinear finite element (FE) studies are used to figure out how RC structures work. The findings show that the dilation angle significantly affects numerical simulation results and intense beam load-displacement behavior. The Finite Element (FE) models' dilation angles offer various behavioral patterns. At a dilation angle of 20°, DB-1 showed a brittle reaction that deviated 39.2% from the intended result. Similar behavior was seen in DB-2. DB-4, with a dilation angle of 56.3, has higher ultimate load capacity and flexibility. This increase did not affect the ultimate load capacity (fu) experimental test results. These results show that the numerical simulation is sensitive to dilation angle alterations, making it crucial for forecasting deep beam structural reactions. The research discovered that the dilation angle substantially impacts the numerical modeling of reinforced concrete deep beams. Specifically, it leads to an increase in the ultimate load capacity and a change towards more ductile behavior as the angle value increases. The work underscores the significance of selecting the appropriate dilation angle to ensure precise numerical simulations that agree with experimental results.

(Hafezolghorani et al., 2017) The study introduces a simplified Concrete Damage Plasticity (SCDP) model for conducting nonlinear analysis on reinforced concrete structures. The tabular model simulates the behavior of unconfined concrete over different grades.

The effectiveness of the SCDP model is evaluated on a prestressed beam, showcasing its accuracy and use in structural engineering applications. The Poisson's concrete ratio varies between 0.1 and 0.2, and the loading history affects the strain changes. The dilatation angle, which impacts the ability of a material to deform without breaking, ranges typically from 20 to 40 degrees. Factors such as plastic strain and restricted pressure influence the internal dilation angle. The material exhibits a consistent dilation angle under different pressure loads. The initial value for the eccentricity of the flow potential is 0.1, and increasing it may enhance the curvature of the flow potential. The CDL model is also used by a more significant number of authors (Bhuiyan & Ahmed, 2022), (Vanova et al., 2023), (Zaioune & Mezhoud, 2023) for their study.

(Najafgholipour et al., 2017) The study analysis the dilation angle in the constitutive equations used in damage plasticity models for concrete materials. The objective is to calibrate the model by conducting sensitivity and mesh sensitivity analysis to evaluate the impact of various logical values of the dilation angle. The dilation angle is essential for accurately representing dilatancy, which refers to the increase in volume under triaxial stress circumstances. The research demonstrates that a higher dilation angle results in greater displacement capacity and the final failure load of the connection. The study suggests that a dilation angle parameter ranging from 31° to 42° is recommended for concrete material. Among these values, 35° is the most appropriate for accurately capturing lateral load-deformation curves and failure modes. This study, using ABAQUS software, aims to enhance constitutive models and optimize material response in concrete under different stress conditions.

(Demir et al., 2018) ABAQUS software was used in a study on numerical modeling of RC deep beam behavior for determining the viscosity parameter's sensitivity. The research verified an experimental investigation using different viscosity parameter values. The aim was to compare the load-displacement behaviors, convergence rate, and calculation time. The findings demonstrated the criticality of the viscosity parameter in numerical simulations of RC deep beams. The research suggests systematically investigating viscosity parameters' sensitivity to identify the most appropriate values.

It identifies values such as 0.0005 as optimal for achieving accurate load-displacement behavior in numerical simulations, consistent with experimental results.

(Najafgholipour et al., 2018) The flexural behavior of lap-spliced reinforced concrete beams under reversed cyclic stress is examined in this work. We compared the standard ACI 318-14 (*ACI CODE-318-14: Building Code Requirements for Structural Concrete and Commentary*, n.d.) design with a modified splice length technique employing 1.25fy on nine full-scale RC beams. The shortened splice length showed superior cyclic performance, surviving cyclic deflections without failures, whereas the traditional design resulted in a semi-brittle failure. The study highlights the significance of altered splice lengths for improved cyclic performance, especially in seismic systems. It is advised that more investigation be done into how splice confinement affects performance under reversed cyclic loadings. These results provide insightful information on seismic design issues and lap splice dependability.

(Mabrouk & Mounir, 2018) A total of sixteen concrete beams were examined under consistent bending moment circumstances. These beams were explicitly chosen for their unique feature of overlapping two bars at the tension side. A comparative study was conducted using the Finite Element Method (FEM) software ABAQUS (*Abaqus 6.14 Documentation*, n.d.). The primary reinforcement comprised two high-quality (400/600) steel deformed bars measuring 10 mm in diameter. ABAQUS utilizes five parameters—K, €, RB/RC, and dilation angle—to fully characterize the plastic behavior of concrete. The default settings specified in the ABAQUS handbook were used. The values are as follows: 2/3 for K, 0.1 for €, 1.16 for RB/RC, and 36 for the dilation angle.

(Nguyen et al., 2020) How couplers affect behavior in reinforced concrete beams with several reinforcing bars is studied. According to experiment data, couplers affect beam bearing capacity, mainly when elastic stage and elastic phase fractures are present. The impact on loading deflection is minimal, 11.25% and 12.25%. The behavior of the beam under static loads is similar to reference beams when coupling reinforcing steel at varying percentages (70.05 to 100%) across the beam length. Coupler number and placement changes affect bearing capacity by 2% to 6%.

A nonlinear finite element analysis using ABAQUS software validates the experimental results. The study shows that simulation techniques can predict and analyze beam behavior with couplers. Still, it also emphasizes the need for more research on coupler effects in reinforced concrete structures using different structural forms and impact load scenarios.

(Rohman et al., 2022) The bond strength between concrete and reinforcement is essential to reinforced concrete sections' structural stability. This study compares the bond strengths of self-compacting (SCC), high-volume fly ash concrete (HVFAC), conventional concrete (NC), and HVFA-SCC. We utilize data from previous research on reinforced concrete beams with lap splicing in the tensile moment region. Normalizing bond strength numbers using the concrete grade's square root simplifies comparison. The study found that HVFAC and HVFA-SCC bind better than SCC and NC. This shows that HVFA-SCC lap splices may be shorter than concrete. Unfortunately, lap splice length code formulations mostly use accurate testing results. Thus, additional research is needed to develop HVFA-SCC-specific formulations. The findings suggest that high-volume fly ash concrete may reduce lap splice length, optimizing reinforced concrete constructions.

(Mustapha, 2023) Analysis and experimentation were used to fix beam precast concrete segment joints—a model estimated rehabilitation flexure capacity for six supported and linked beams. The key finding is that casting NSC or HSC alone in the connecting zone does not increase beam capacity. CFRP laminates and warped fiber sheets increased load capacity by 122% and 209% over NSC and HSC beams, respectively. The recommended model based on CNR-DT 200 R1/2013 accurately assessed fixed connection capacity using CFRP laminates and warped fiber sheets. Specific rehabilitation procedures are crucial for realistic beam-to-beam connection improvements.

(Haavisto et al., 2023) Enhancing structural flexibility in plastic hinge development zones is a critical structural engineering issue in reinforced concrete beams with lap splices. This study is essential since Eurocode EC2 (Eurocode 2: Design of Concrete Structures | Eurocodes: Building the (Future, n.d.) is being changed. It provides valuable information that may enhance reinforced concrete structure design.

The experimental campaign carefully evaluates lap lengths, bar diameters (12–25 mm), and reinforcement percentages on 38 specimens in four-point bending. The fundamental discovery is that lap lengths beyond bar yielding dramatically enhance structural ductility. This suggests a lap length multiplying factor, giving designers a helpful rule of thumb. The study provides data and a speculative model for bond-stress distribution in lap splices post-bar yielding. This work improves our understanding of lap splice behavior, impacts the future Eurocode revision, and enhances efforts to strengthen reinforced concrete structure seismic resilience.

2.4 Summary

This chapter overviews previous efforts, illuminating the substantial research on Reinforced Concrete (RC) beams, particularly emphasizing Normal Strength Beams. This text thoroughly explores the benefits and drawbacks of these beams, offering valuable insights derived from previous research. An essential feature of this topic is the vital connection between the values derived by ABAQUS, a Finite Element Analysis (FEA) software, and the equivalent experimental values of RC beams. The chapter highlights the importance of using ABAQUS for this purpose, explicitly stressing its role in clarifying the behavior of RC beams using Finite Element Analysis (FEA). In addition, the chapter discusses the consequences of the failure parameter. It provides valuable information on the decision-making process that led to the selection of ABAQUS as the appropriate instrument for this research.

CHAPTER 3
MODELING & ANALYSIS

3.1 Introduction

This chapter covers a comprehensive overview of the sample beams, containing all of the material properties and particular specifications. These beams were thoroughly prepared using AutoCAD 2024 (*AutoCAD 2024 Help | Autodesk*, n.d.) and FEA software, ABAQUS 2017 (*Abaqus 6.14 Documentation*, n.d.). The chapter includes step-by-step instructions for completing the FEA procedure and outlining the model's specifics. (Mabrouk & Mounir, 2018) The researcher conducted experimental testing on 18 beams, meticulously validating the experimental results using the ABAQUS environment. The beams were tested in various situations, including scenarios with and without lap splices, varied stirrup shapes, changing numbers of transverse reinforcement, and multiple types of concrete. The beams had specified 2000 × 250 × 150 mm (Mabrouk & Mounir, 2018). Our study mainly addresses three beams, focusing on essential factors for analysis, such as material characteristics, compression angle, viscosity, and the effect of the mesh size. The studies were performed using the advanced finite element program ABAQUS.

3.2 Specifications of the specimen

All three beams have the exact dimensions of 2000 x 250 x 150 mm, which ensures stability and allows a controlled comparison throughout the numerical analysis. The consistent dimensions of these beams allow for a systematic comparison, enabling a thorough analysis of their reactions under various conditions. The uniformity in beam size enhances the reliability of the numerical analysis, providing an adequate basis for evaluating and contrasting the efficiency of different beam categories. The left side of each beam is supported by a spring with a length of 100 mm, while the right side is supported by a roller with a height of 100 mm. These supports play a role in determining the overall structural behavior. The Figure (Fig. 3.1) displays a comprehensive 2D representation of a concrete beam.

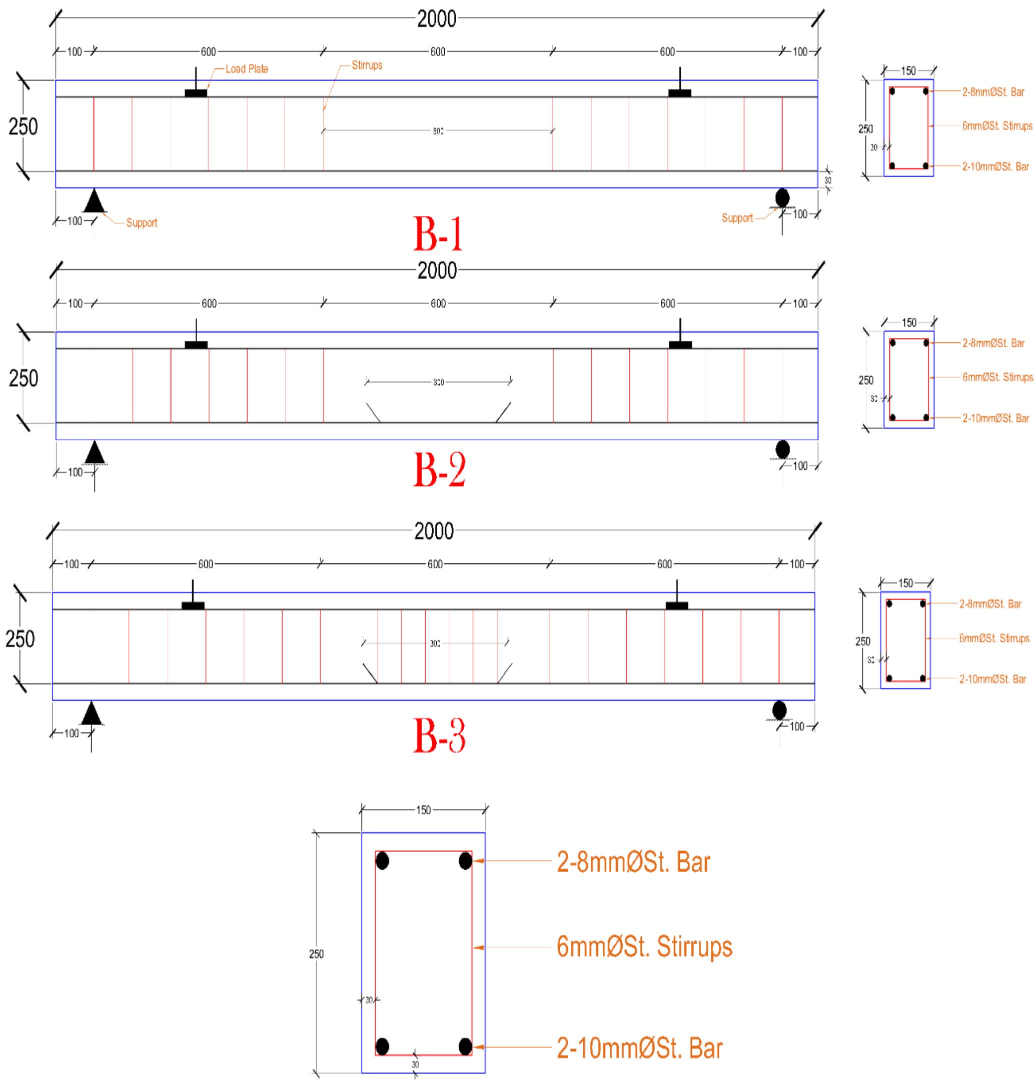

Fig. 3.1: 2D View of Specification of the Specimen (AutoCAD).

Each beam has two loading plates that are appropriately linked to the top surface of the beam, allowing the beams to respond differently to varied loads. The top bar comprises reinforcing bars with a diameter between 2 and 8 millimeters. Reinforcing bars with diameters varying from 2 to 10 millimeters make up the bottom bar portion of the structure. Stirrups: Make sure all the beams have lateral reinforcement using stirrups with a diameter of 6 millimeters. For every one of the beams, we used a vertical shape. The nominal thickness of the transparent cover on both sides is thirty millimeters.

3.2.1 Specifics of the beam:

This investigation investigates the structural reaction of three reinforced concrete beams (B1, B2, and B3) with varied configurations using finite element analysis (FEA) in ABAQUS. The study also evaluates the impact of lap splicing and transverse reinforcement on the structural response. Considering the influence that the shape of the stirrups and the amount of transverse reinforcement have on the overall design. The beams in the investigation are methodically designated to ensure clarity:

B1 (NC-L00-0T6): This beam, referred to as NC (Normal Strength Concrete), L00 (without lap splice), 0T6 (without transverse reinforcement and with 6 mm diameter for stirrups), serves as a reference for analysis. In the absence of a lap splice, stirrups, or transverse reinforcement in the central section (600 mm), it enables the evaluation of structural performance without particular reinforcing elements.

B2 (NC-L30-0T6): This beam has a lap splice without transverse reinforcement in the splice zone (600 mm), and it is identified as NC (Normal Strength Concrete), L30 (lap splice of 300 mm), and 0T6 (no transverse reinforcement and 6 mm diameter for stirrups). This setup requires a separate reinforcing criterion for assessment.

B3 (NC-L30-6T6): This beam, which is also identified as NC (Normal Strength Concrete), L30 (lap splice of 300 mm), and 6T6 (6 transverse reinforcement and 6 mm diameter for stirrups), has a lap splice with transverse reinforcement in the splice zone (600 mm). The design enhances the state, making comparing and analyzing the structural behavior easier.

The material provided includes the particular dimensions, support conditions, loading configuration, and reinforcing details for each of the three beams (B1, B2, and B3) used in the numerical analysis performed using ABAQUS. A concrete beam is shown in a three-dimensional view using ABAQUS, as shown in the Figure below (Fig. 3.2).

a) **b)**

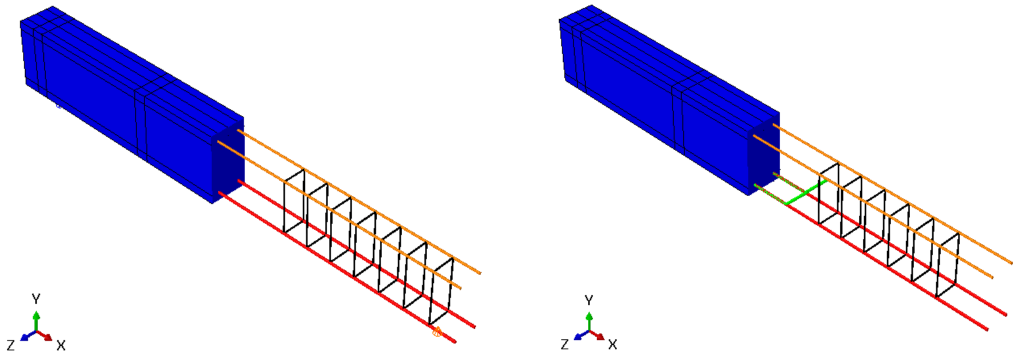

c)

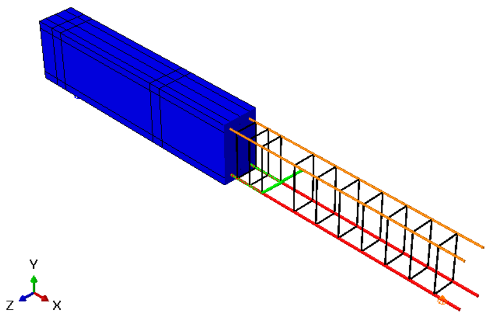

Fig. 3.2: 3D View of Concrete beam of a) B1, b) B2, c) B3 using (ABAQUS).

3.3 Reinforcement Concrete Beam

Beams made of reinforced concrete are structural components specifically intended to handle external loads perpendicular to the beams. These beams generate bending moment, shear forces, and torsion. As a result of concrete's great compressive strength but poor tensile strength, steel reinforcing is required to counterbalance the effects of tensile stresses. The weight of the slabs, other beams, walls, and columns are carried by these beams and transmitted to the columns supporting the structure. In addition, they may be built in various forms, including rectangular, square, T-shaped, or L-shaped portions. A single or double reinforcing method may be used for beams. A three-dimensional reinforced concrete beam that was chosen at random is shown in the following Figure (Fig. 3.3).

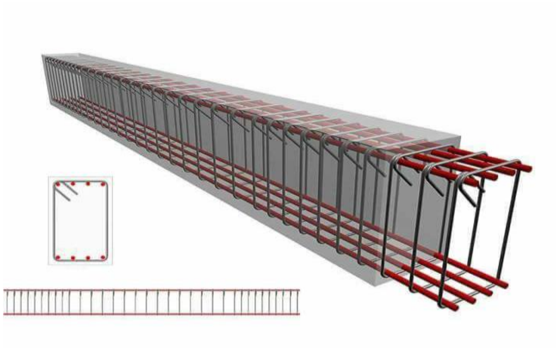

Fig. 3.3: 3D View Detail of a Reinforced Concrete Beam

3.4 Material Property

This study aims to clarify the experimental verification of reinforced concrete (RC) beams using Finite Element Analysis (FEA) software, specifically focusing on understanding the impact of failure factors. The main incentive is to meet the urgent requirement for precise and dependable techniques to evaluate the structural performance of reinforced concrete beams, which is essential for guaranteeing their safety and effectiveness. Three separate beams were experimentally tested with different parameters to achieve this objective, as shown in the table (Table 3.1: Material Properties (Mabrouk & Mounir, 2018). The project also entails utilizing FEA software to simulate and forecast the behavior of reinforced concrete beams, implementing consideration of the impact of failure properties.

Table 3.1: Material Properties (Mabrouk & Mounir, 2018).

Beam No	Concrete Type	Concrete Strength (MPa)	Steel Strength (MPa)	Modulus of Elasticity of Concrete (GPa)	Modulus of Elasticity of Steel (GPa)
B-1	Normal Strength	31.86	400	28.4	210
B-2	Normal Strength	30.67	400	26.86	210
B-3	Normal Strength	32.56	400	28.7	210

3.4.1 Concrete Property

The critical material parameters, such as the compressive strengths of concrete and Poisson's ratio, are essential factors in determining the structural response of the beams under different loading circumstances.

The investigation included three control specimens, each constructed from three different types of concrete: Normal Strength Concrete (NC), High Strength Concrete (HC), and Self-Compacting Concrete (SC). However, in our study, all three beams were always made with normal-strength concrete. This gave us a uniform and focused way of looking at things.

3.4.1.1 Concrete Damage Plasticity

Concrete damage plasticity is a method used in ABAQUS to precisely simulate the nonlinear behavior of concrete structures by employing constitutive modeling techniques. The method includes damage variables to measure the deterioration of materials, enabling a thorough depiction of plastic deformation and damage buildup.

(Mabrouk & Mounir, 2018)The concrete damaged plasticity model was used in this work because it correctly shows the complete non-elastic behavior of concrete, including tension-compression and damage features. This model suggests that concrete might fail in two ways: forming cracks under tension and collapsing the material under compression. The stress-strain relationship for concrete under compression demonstrates a first linear-elastic phase that extends up to 30–40% of its compressive strength.

After this point, it shifts into a plastic behavior, as seen in Figure (Fig. 3.4). This model offers a thorough depiction of the mechanical behavior of concrete under different loading circumstances.

The dilation angle measures the increase or decrease in volume due to stress, while eccentricity quantifies the displacement between applied loads and the central axis of structural components. ABAQUS incorporates viscosity as a material property, allowing for the representation of time-dependent phenomena and dynamic responses in structural analyses. The optimum dilation angle parameter for concrete materials is from 31° to 42°, whereas the optimum Kc value ranges from 0.5 to 1. By changing the viscosity on purpose, we can look at how it affects the beams' response during the analysis in a planned way. This gives us helpful information about viscosity's role in the structure's behavior, as described in the next chapter of this study.

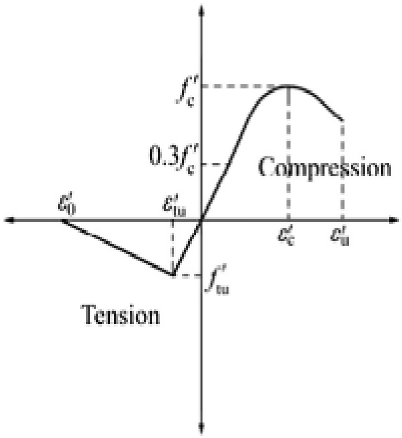

Fig. 3.4: Typical concrete stress-strain curves (Mabrouk & Mounir, 2018).

To validate our Finite Element Analysis (FEA), we provided concrete compressive strengths of 31.86 MPa, 30.67 MPa, and 32.56 MPa to Beams B-1, B-2, and B-3, respectively. These beams are all classified as normal-strength concrete. The concrete Poisson's ratio was uniformly established at 0.2 to provide uniformity across all beams. The Figure (Fig. 3.6) below demonstrates these features, briefly describing the allocated material properties for each beam.

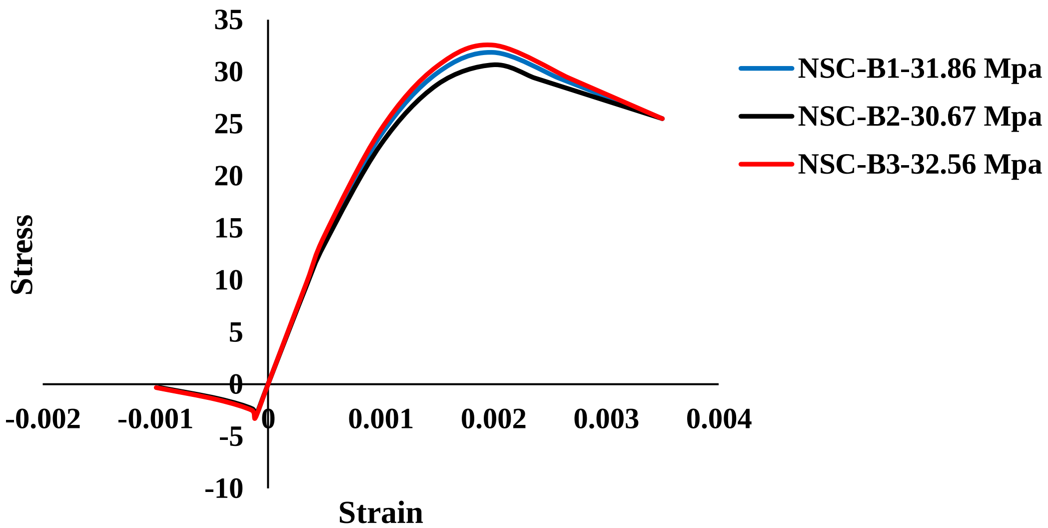

Fig. 3.5: material property of concrete for RC beams.

3.4.2 Steel Property

The primary reinforcement used in the investigation consisted of two high-quality (400/600) steel deformed bars with a diameter of 10 mm. The reinforcing steel was assumed to have elastic-perfect plastic behavior in tension and compression.

The behavior of steel in the elastic zone was represented as linear and isotropic in ABAQUS, with the modulus of elasticity and Poisson's ratio given to ensure the correct simulation of flexible behavior. However, after the stress in the steel exceeded the yield stress, irreversible plastic deformation began, leading to a reduction in steel rigidity. The reinforcing steel followed the stress-strain curve specified in Eurocode 2 1992-1(*Eurocode 2: Design of Concrete Structures | Eurocodes: Building the Future*, n.d.), as shown in (Fig. 3.6) (Mabrouk & Mounir, 2018). This method enabled a thorough depiction of the mechanical behavior of the reinforcing steel throughout the loading procedure.

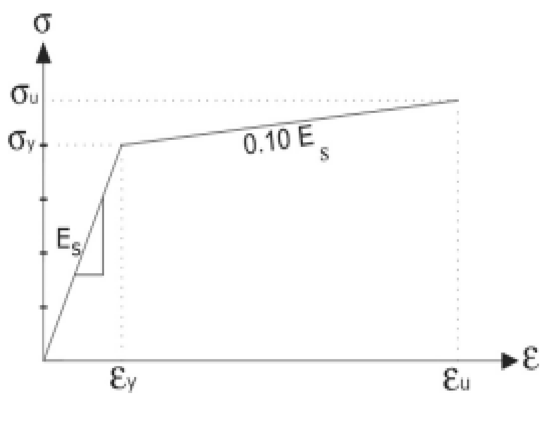

Fig. 3.6: Diagram for the design of stress and strain in reinforcing steel (Mabrouk & Mounir, 2018).

When completing our Finite Element (FE) study, we employed the same material characteristics regardless of whether we conducted parametric or validation investigations. The yield strength of the steel that was utilized is 400 megapascals. Concrete of a normal strength served as a representation of the substance that was being investigated. It was determined that a Poisson ratio of 0.3 for elastic steel was employed regardless of the conditions.

Normal-strength concrete and a uniform steel Poisson ratio provide a standardized method for assessing the structure's reaction to various loading conditions. This method is used throughout the research phase. 400 MPa Steel makes it possible to reflect the natural world's behavior correctly, and the constant Poisson ratio simplifies the material characterization process and the following analysis. For every one of those qualities, Figure 3.4 illustrates.

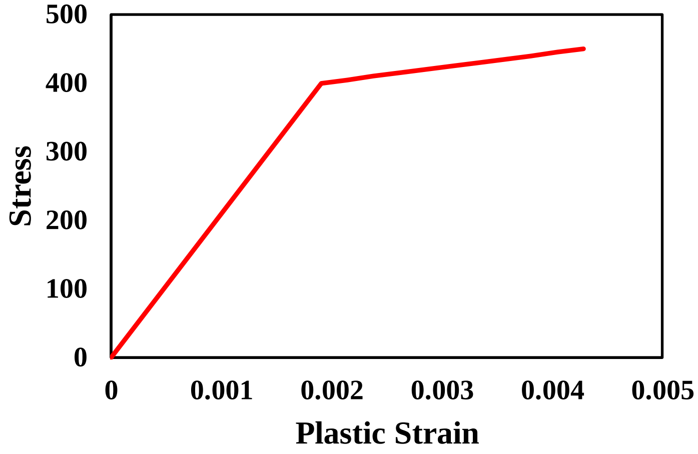

Fig. 3.7: Material properties of steel reinforcement

3.5 Analytical procedure

The study uses ABAQUS for reinforced concrete beam finite element analysis. Geometric and material parameters like dilation angle, viscosity, and mesh density are defined first. To discretize the model, (C3D8) for concrete and (T3D2) for reinforcement are used. Meshing is vital, and mesh sizes are evaluated. The work sets boundary conditions and loads utilizing rigid and loaded plates to imitate real-life settings. Concrete damage plasticity, dilation angle, and viscosity are examined. Explore dilation angle, viscosity, steel quality, and mesh density variations. Model validation is essential to guarantee that numerical simulations match experimental data. The paper closes with a detailed investigation of finite element models, examining how factors affect reinforced concrete beam structural behavior.

3.5.1 Steps of the model

A summary of all the modeling and analysis phases is provided in the flow chart (Fig.3.4) below.

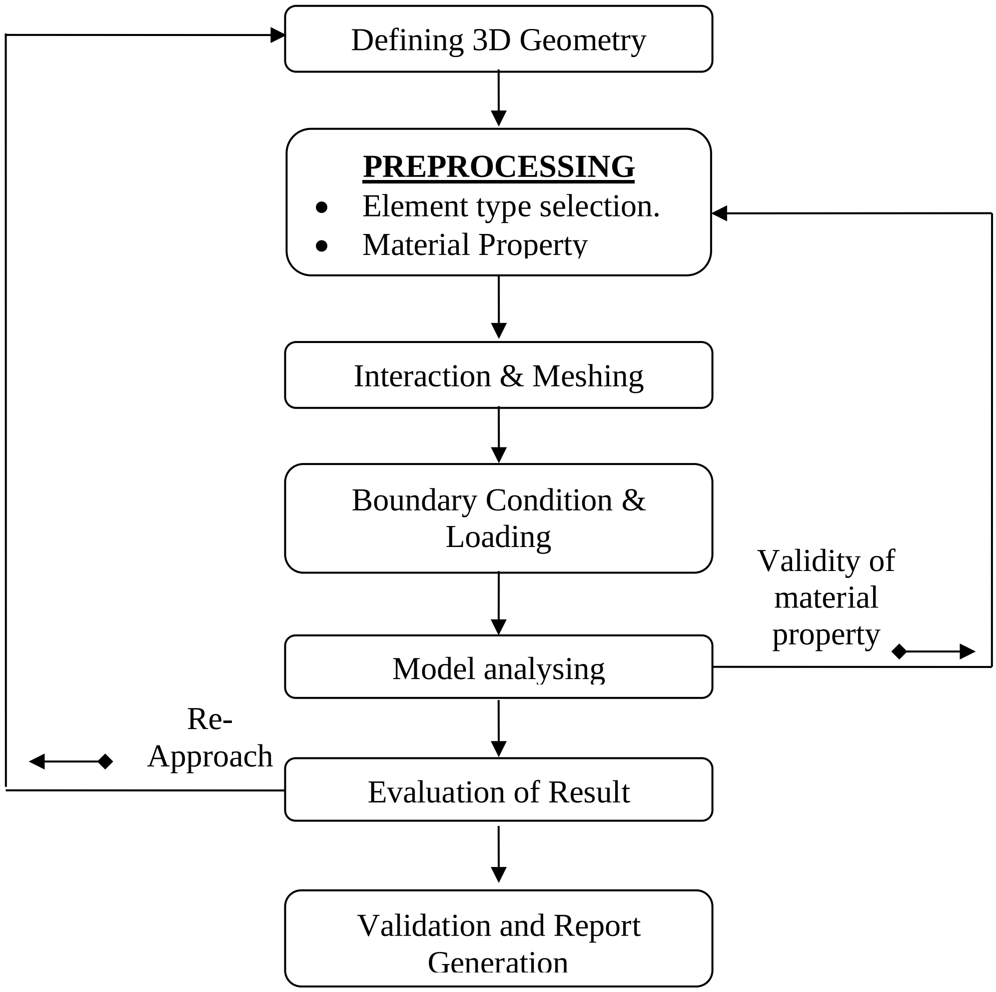

Fig. 3.8: Steps in modeling and analysis

3.5.2 Element Type

The modeling approach in this section utilizes an eight-nodded continuum solid element known as C3D8 (Fig: 3.9A). The C3D8 element models the concrete part of reinforced concrete (RC) structures. It represents a 3D stress 8-node linear brick. In addition, a two-node linear 3D truss element, known as T3D2 (Figure 3.9B), represents the reinforcement in the reinforced concrete structure. The T3D2 element models a 3D truss with two nodes and linear behavior.

The size of the elements used to discretize the structure is a crucial factor in Finite Element (FE) analysis. The figure (Fig. 3.10) Shows the 3D View of the Type of the element. The accuracy of the analysis results directly depends on the selected element sizes. When analyzing the structure, more minor elements, particularly deflection and force, lead to more precise outcomes. Thoroughly assessing the sizes of elements is crucial for attaining dependable and accurate outcomes in the FE analysis.

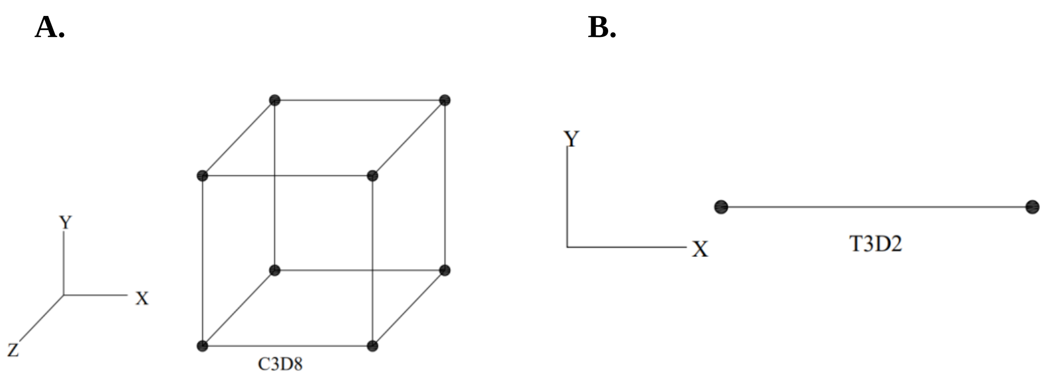

Fig. 3.9: A & B Types of elements used to model by ABAQUS (2017).

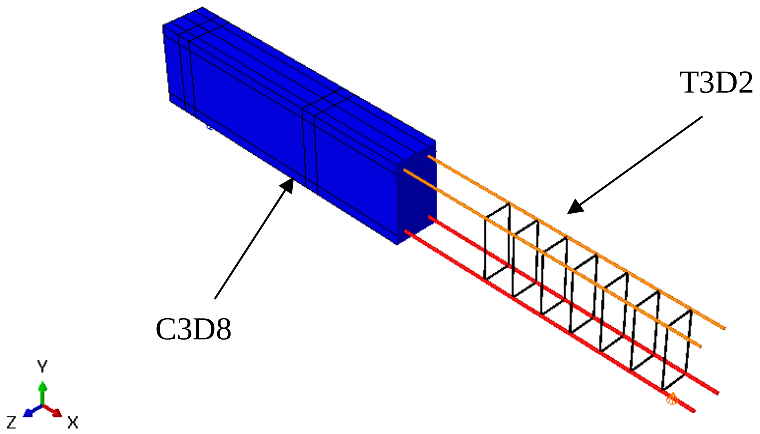

Fig. 3.10: Type of the element

3.5.3 Interaction Across Elements

This model exhibits interconnectivity between two parts, resulting in a cohesive structural depiction. The T3D2 element, representing a two-nodded linear 3D truss, is incorporated into the C3D8R material element, meaning a three-dimensional stress eight-nodded linear brick.

This connection improves the model's accuracy, enabling a thorough simulation of the interaction between the truss-type reinforcement and the concrete material.

The ABAQUS model used the 'embedded' approach to establish the connection between the reinforcement and concrete. This included categorizing the steel reinforcement as the embedded component and the concrete as the host component. This method provides an accurate portrayal of the interaction between the two substances.

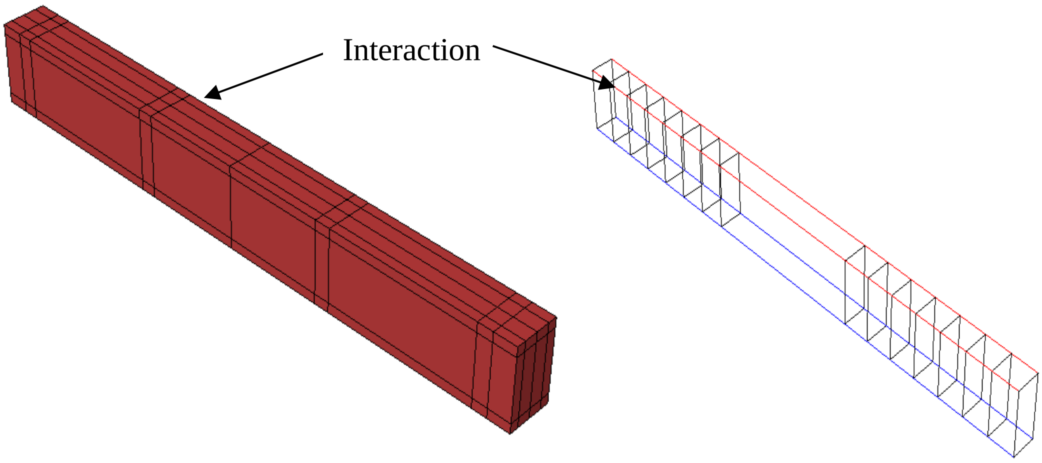

Fig. 3.11: Interaction of RC Beams in FEA.

Incorporating these components allows for a more accurate depiction of the highly complex behavior of the reinforced concrete structure under different loading conditions, including the interaction between the individual reinforcement and the uninterrupted factual matrix. The purpose of this arrangement was to accurately replicate the actual interaction between concrete and steel, guaranteeing the precision and dependability of our simulation findings.

3.5.4 Meshing

Meshing is a crucial step in finite element analysis (FEA), where complex geometry is divided into smaller, simpler components to facilitate a numerical estimate of its behavior under different conditions.

Converting the ongoing physical model into a discrete mathematical representation is essential to ensure the precision and effectiveness of simulations. Precise and linked models allow the software to mimic the structural reaction accurately, providing significant insights into the system's behavior under different loads and boundary conditions. Meshing is a crucial procedure in analysis that ensures the precision and reliability of numerical simulation results. During our study, we developed six distinct versions of meshes for each beam. The mesh sizes ranged from 15 to 50 millimeters, with increments of 5 millimeters. This topic will be covered in the next chapter.

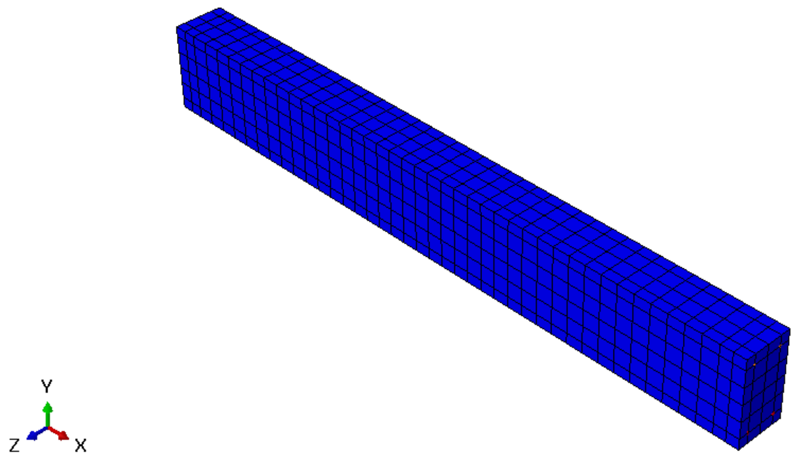

Fig. 3.12: 3D RC beam mesh size analysis.

3.5.5 Boundary Conditions

In ABAQUS, defining border conditions means naming constraints like supports, and defining loads means calling outside forces or conditions that act on the structure. ABAQUS provides an intuitive interface for correctly simulating real-world situations, enabling exact specifications of restrictions, displacements, and rotations. Accurate simulation results in ABAQUS rely on well-defined boundary conditions and loading, essential for capturing realistic structural reactions and gaining valuable insights into system behavior. For our simulation, we replicated the actual experimental circumstances by using four rigid plates of solid parts to support the beams. The constraints, known as "Tie," were established to provide a rigid connection between the support and loading plates, thereby limiting any movement between the beam and the plates.

While the loading was not directly allocated to the beam, the load from the loading plate was efficiently transmitted to the specified location on the beam. The rigid loading plates were used to prescribe displacement in the RC beam. These plates were positioned at the load plate of the beam and allowed movement only in the vertical direction.

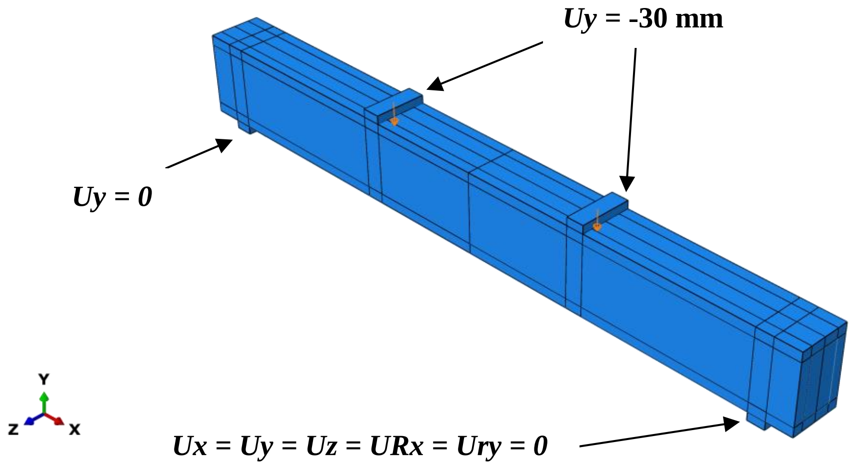

Fig. 3.13: Loading & Boundary Condition

Each beam is supported on the left side by a spring measuring 100 mm long and on the right side by a roller measuring 100 mm long. These supports contribute to the determination of the overall structural behavior.

3.6 Summary

This chapter discusses the beam specifications, including material parameters, the application of concrete damage plasticity, the selected model type, the specimen profile, load considerations, boundary conditions, and the specifics of the model meshing. Our research utilizes two widely used software tools, AutoCAD 2024 (*AutoCAD 2024 Help | Autodesk*, n.d.) and ABAQUS (2017) (*Abaqus 6.14 Documentation*, n.d.), for design and analytical purposes. The next chapter concludes with a complete review of the study's procedures and results after successfully analyzing these finite element models.

CHAPTER 4
Result and Discussion

4.1 Introduction

The study included the analysis of three beams with different mesh and viscosity characteristics. The aim was to rebuild the reinforced concrete beam using the same material properties specified in the previous section. This section will provide a more comprehensive examination of the material characteristics used in our modeling studies. Following that, we will focus on the results and outcomes of the analysis, offering a complete knowledge of the behavior of the reinforced concrete beams under different conditions. This chapter thoroughly examines the extensive findings obtained by analyzing different types of beams. We closely discuss the effects of dilation angle, viscosity variations, mesh size influence, and error assessment in determining ultimate failure loads in experimental and ABAQUS analyses. The results comprehensively comprehend the structural behavior under various settings, providing valuable insights into the performance of the beams and the efficacy of the applied parameters. The chapter offers a vital platform for examining the research's subtle components, revealing each variable's complexities and impact on the overall structural response.

4.2 Validation of Finite Element Models

Validating finite element models is essential to guarantee the precision and dependability of structural examinations. The process entails comparing Finite Element Analysis (FEA) predictions with empirical data to detect disparities and evaluate the model's efficacy. The procedure involves sensitivity analysis to assess the influence of parameter adjustments on the prediction skills. Validation increases the reliability of FEA results, making the models more resilient and efficient for influencing design and analysis choices in structural engineering. The validation procedure will mainly focus on the impacts of several parameters, such as dilation angles, viscosity, steel grade, meshing, and the modulus of elasticity of steel.

Through a systematic investigation of numerous factors like dilation angle, viscosity, and mesh size, we aim to evaluate the accuracy and responsiveness of the model under different circumstances. Our objective is to achieve a thorough validation process by systematically adjusting these factors and comparing the findings of Finite Element Analysis (FEA) with empirical data. This rigorous technique improves our comprehension of the model's behavior across various circumstances, confirming its dependability in precisely forecasting the structural reaction of reinforced concrete beams.

4.2.1 Validation parameter based on Dilation angle

During the validation phase, many experiments were performed to evaluate the influence of various dilation angles on the structural response of reinforced concrete beams. The dilation angle, an essential measurement in our investigation, usually ranges from 30 to 40 degrees. This specific range has been meticulously selected to include a broad variety of values, enabling a complete examination of its impact on structural behavior. By examining this wide array of options, our objective is to comprehend the subtle variations in the reaction of the beams when subjected to different degrees of expansion, therefore enhancing our comprehension of their overall effectiveness. The dilation angles of 39, 37, 36, 32, and 31 were investigated in multiple model analyses. The figure below (Fig. 4.1) illustrates the variation in the dilation angle while maintaining a constant viscosity of 30%, using steel grade 400/450 and a mesh size of 25mm. The figure ψ means the dilation angle. The primary objective was determining the ideal dilation angle that consistently matched the expected structural reactions. A thorough analysis of the experiment results concluded that a dilation angle of 31 degrees displayed the most appropriate relationship with the structural behavior that was explicitly wanted. Consequently, this particular angle was selected to serve as the standard dilation angle for all the beams included in the study.

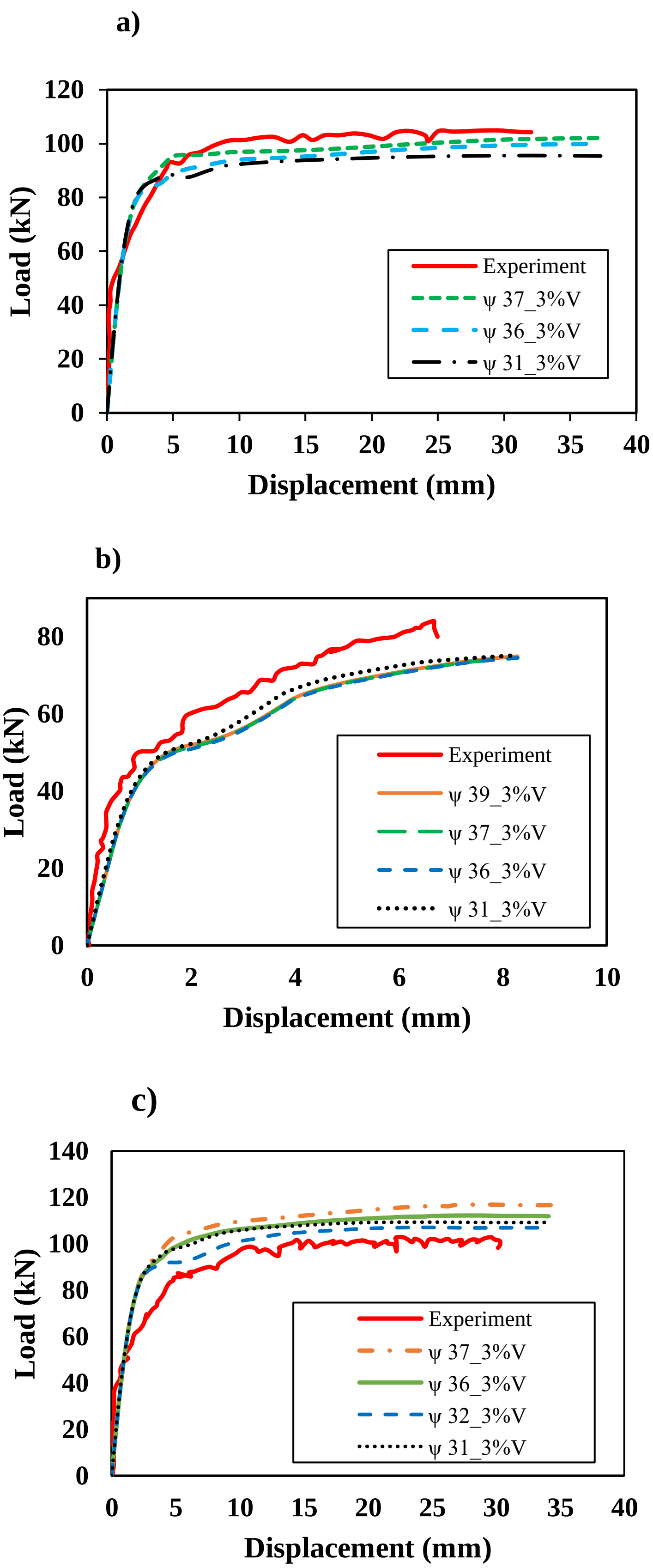

Fig. 4.1: Load vs. displacement validation-based dilation angle for a) B-1, b) B-2 and c) B-3

4.2.2 Viscosity-based validation parameter

The validation's purpose was to ensure that the chosen viscosity values correspond with the empirical data and appropriately illustrate the structural behavior of the reinforced concrete beams. The detailed documentation of the findings and specifics of each viscosity experiment performed throughout the validation phase provides a solid basis for the dependability of the finite element analysis model.

This study examines the effect of varied viscosity percentages on structural responses using different values for beams B1, B2, and B3. Within the scope of our investigation, the consideration of viscosity was carried out using a systematic methodology. The study included several trials, with the viscosity value initially set at 0.0001 for all beams, resulting in a protracted procedure. The succeeding procedures gradually raised the viscosity value to simplify and expedite the study. Using an iterative approach, a range of viscosity was determined, ranging from 1% to 10%, to enhance the study's efficiency while preserving accuracy.

The illustration shown in Figure (Fig. 4.2) clearly illustrates the impact of viscosity changes on the beams' structural behavior, where V denotes viscosity. A comprehensive record of each viscosity test is included in the appendix to provide a point of reference. The graph below indicates the best viscosity values in conjunction with a dilation angle of 31 degrees. This combination is highlighted as the influential combination that results in a structural response in the beams.

During an in-depth study, the viscosity percentages found to be most appropriate for each beam were 0.04 for beam B1, 0.05 for beam B2, and 0.025 for beam B3. The selected mesh size, an important aspect affecting accuracy, was maintained identically at 25 millimeters. Using a comprehensive study of changes in viscosity may improve the accuracy of finite element models. This is accomplished by ensuring that the chosen viscosity values are compatible with other factors, enhancing the overall precision of structural assessments.

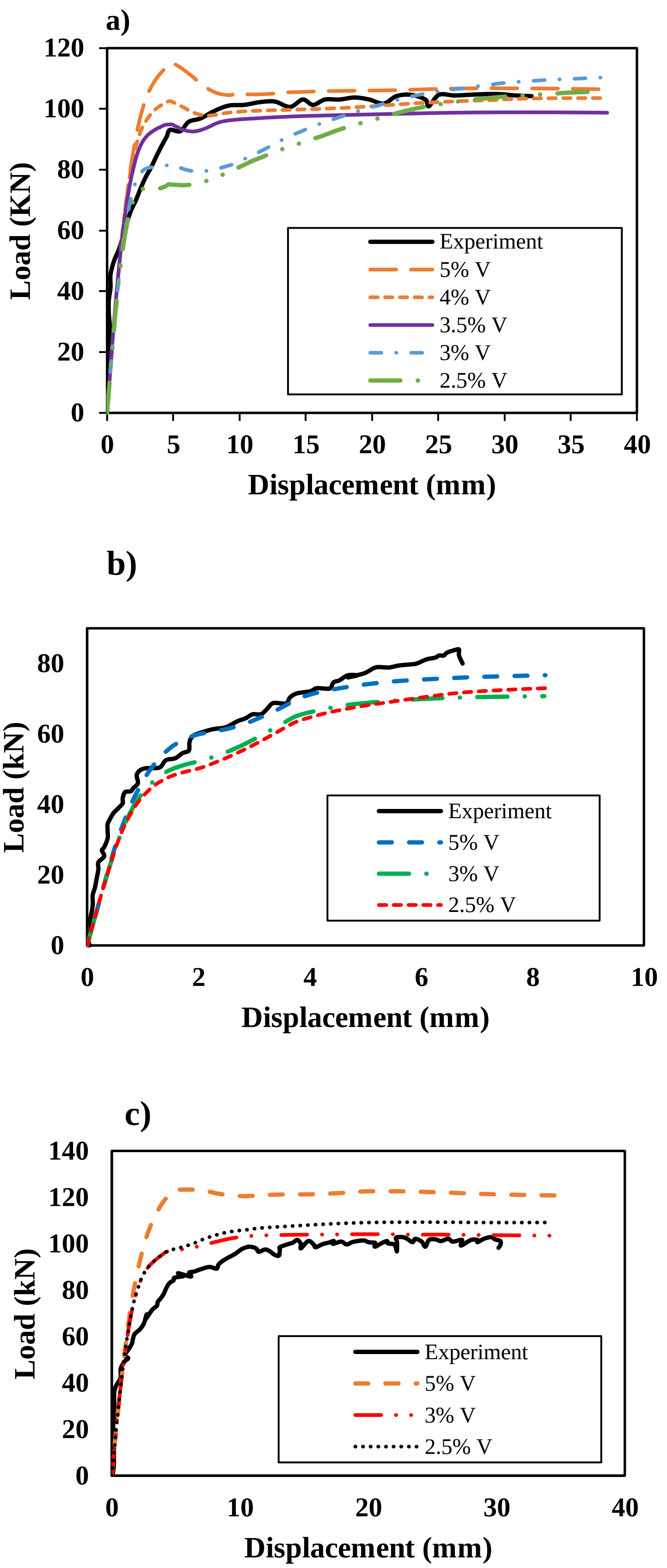

Fig. 4.2: Viscosity Variation for a) B-1, b) B-2 and c) B-3

4.2.3 Verification of the Mesh in Finite Element Models

Meshing is an essential process in finite element analysis (FEA), where a complicated structure is divided into smaller connected parts. Combining these parts creates a mesh, allowing for modeling structural behavior using mathematical equations at specific nodes. The technique has a substantial impact on both the accuracy and computing efficiency of the study.

To achieve optimal meshing, a more excellent mesh resolution is sacrificed to increase accuracy, whereas a lower mesh resolution is offered to improve computing efficiency. Because of this, the simulation results for structural models used in various engineering applications are guaranteed to be reliable.

There is a clear relationship between the size and quality of the mesh and the accuracy of the conclusions gained by FEA. Although the system's accuracy is improved by using smaller components, the amount of computational work that must be done also increases. The suitable meshing approach perfectly balances accuracy and processing efficiency, providing reliable simulations of the behavior of structures under various circumstances. When doing finite element analysis (FEA), it is essential to have a mesh that is well specified to get relevant results and insights on the performance of structures.

In the study, we used six different mesh sizes, namely 15, 20, 25, 30, 40, and 50 millimeters, to evaluate the influence of these sizes on each beam's structural behavior. After completing an intensive analysis, we understood that the outcomes achieved from these varied mesh designs were equivalent, with just a tiny difference between them. Our study used a mesh size of 25 for every beam. This was because we discovered that varied mesh sizes gave comparable results. Because of this choice, which finds a balance between the efficiency of computing and the accuracy of the findings, it is suitable for capturing the structural behavior that is being researched. Our study used a wide range of mesh sizes, as shown in the illustration below (Fig. 4.3: Different types of Mesh Size a) M 50mm b) M 40mm c) M 30mm d) M 25mm e) M 20mm f) M 15mm).

a) **b)**

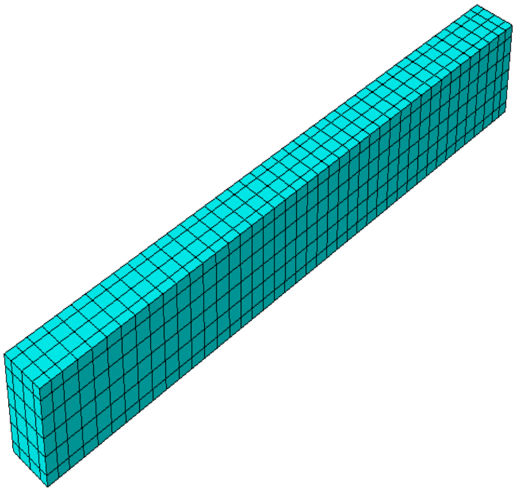
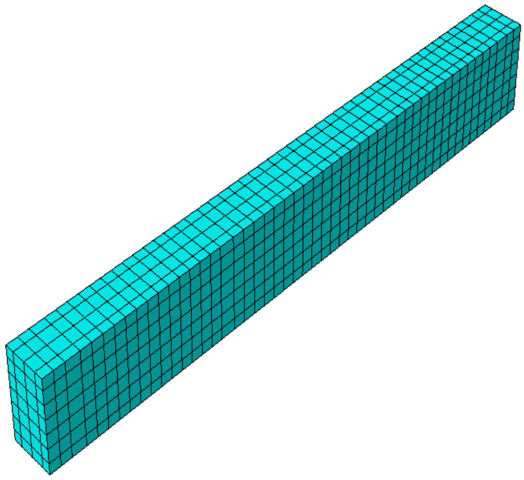

c) **d)**

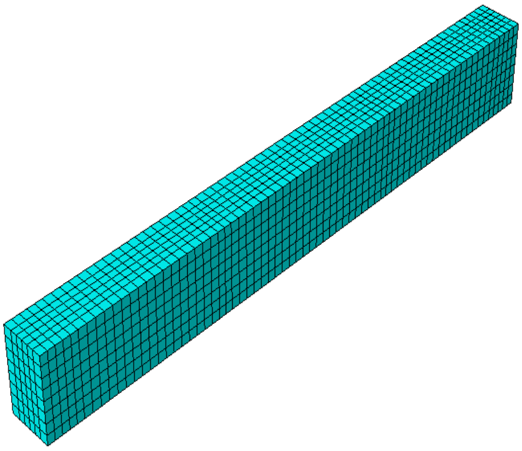
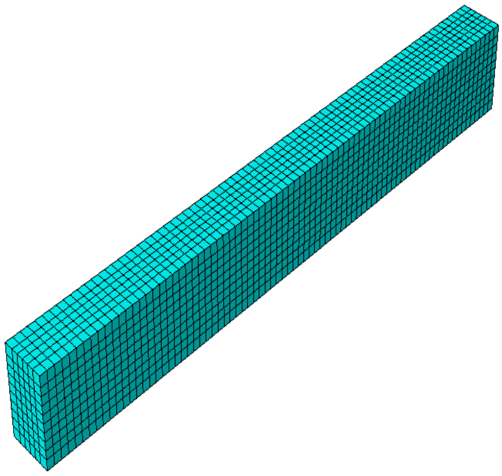

e) **f)**

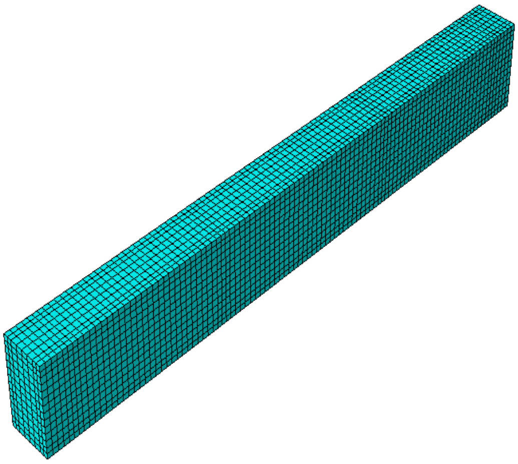
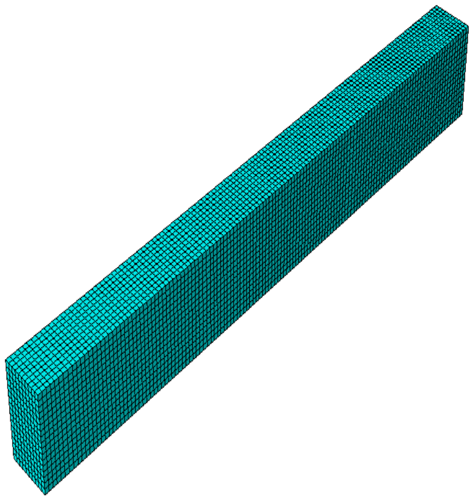

Fig. 4.3: Different types of Mesh Size a) M 50mm b) M 40mm c) M 30mm d) M 25mm e) M 20mm f) M 15mm

4.2.3.1 Various validation assessment

We performed a comprehensive analysis in our investigation, using several trials to improve the accuracy of our beam assessments. The Appendix section will provide a complete presentation of the specific findings, including the differences in load between the experimental and ABAQUS outcomes for each trial. This will thoroughly review the performed trials and their respective outcomes. A summary of the trials and errors for each beam, for B-1 trails, and the error table (Table 4.1) is shown in the table below. The maximum load capacity of the experiment is 105 kilonewtons.

Table 4.1: Trials and errors for B-1

Trials	D-V-M	FEA	Error %	Trials	D-V-M	FEA	Error %
J 1	36-0.03-25	113.27	7.88	**J 21**	37-0.03-25	99.13	5.59
J 2	36-0.03-25	108.30	3.14	**J 22**	37-0.03-25	102.09	2.77
J 3	36-0.3-25	415.29	295.51	**J 23**	36-0.05-25	127.08	21.03
J 4	36-0.3-25	399.06	280.06	**J 24**	36-0.03-25	97.58	7.07
J 5	31-0.03-25	104.83	0.16	**J 25**	31-0.05-25	114.86	9.39
J 6	31-0.03-25	110.36	5.10	**J 26**	31-0.03-25	89.79	14.49
J 7	36-0.025-25	108.32	3.16	**J 27**	31-0.025-25	90.06	14.23
J 8	36-0.025-25	105.90	0.86	**J 28**	36-0.025-25	91.05	13.29
J 9	31-0.025-25	105.83	0.79	**J 29**	31-0.025-25	106.10	1.04
J 10	31-0.025-25	101.75	3.10	**J 30**	36-0.025-25	107.60	2.48
J 11	37-0.03-25	117.32	11.73	**J 31**	31-0.03-25	95.56	8.99
J 12	37-0.03-25	113.33	7.93	**J 32**	31-0.05-25	114.86	9.39
J 13	37-0.025-25	111.03	5.74	**J 33**	**31-0.04-25**	**103.57**	**1.36**
J 14	37-0.025-265	107.17	2.07	**J 34**	31-0.035-25	98.90	5.81
J 15	37-0.03-25	116.22	10.69	**J 35**	31-0.04-15	101.54	3.30
J 16	36-0.03-25	114.80	9.33	**J 36**	31-0.04-20	103.45	1.48
J 17	36-0.03-25	116.86	11.30	**J 37**	**31-0.04-30**	**105.66**	**0.63**
J 18	36-0.03-25	105.63	0.60	**J 38**	31-0.04-40	109.16	3.96
J 19	36-0.03-25	100.00	4.76	**J 39**	31-0.04-59	109.75	4.52
J 20	36-0.03-25	97.09	7.53				

The optimal mesh size for B-1 is **30mm**, but the typical mesh size is **25mm**.

In the following table, we will discover a summary of the trials and errors that occurred for each beam, as well as for the B-2 trials and the error table (Table 4.2). Eighty-four (84) kilonewtons is the highest load capacity the experiment can support.

Table 4.2: Trials and errors for B-2

Trials	D-V-M	FEA	Error %	Trials	D-V-M	FEA	Error %
Job 1	37-0.03-25	74.48	11.33	**Job 17**	36-0.03-25	79.49	5.37
Job 2	36-0.03-25	74.52	11.29	**Job 18**	36-0.03-25	71.69	14.65
Job 3	39-0.03-25	74.93	10.80	**Job 19**	31-0.03-25	76.68	8.71
Job 4	37-0.03-25	75.72	9.86	**Job 20**	31-0.03-25	70.74	15.79
Job 5	39-0.03-25	74.98	10.74	**Job 21**	31-0.03-25	73.01	13.08
Job 6	37-0.03-25	70.90	15.60	**Job 22**	36-0.03-25	75.41	10.23
Job 7	36-0.03-25	72.36	13.86	**Job 23**	31-0.03-25	74.56	11.24
Job 8	36-0.03-25	69.85	16.85	**Job 24**	36-0.03-25	76.39	9.06
Job 9	36-0.03-25	76.23	9.25	**Job 25**	31-0.03-25	75.14	10.55
Job 10	31-0.03-25	68.37	18.61	**Job 26**	**31-0.05-25**	**80.88**	**3.71**
Job 11	37-0.03-25	74.22	11.64	**Job 27**	31-0.05-15	79.98	4.79
Job 12	31-0.03-25	67.90	19.17	**Job 28**	31-0.05-20	80.59	4.06
Job 13	31-0.03-25	75.92	9.62	**Job 29**	31-0.05-30	82.65	1.61
Job 14	36-0.03-25	77.88	7.29	**Job 30**	31-0.05-40	83.51	0.58
Job 15	36-0.03-25	78.87	6.11	**Job 31**	**31-0.05-50**	**84.30**	**0.36**
Job 16	36-0.03-25	79.37	5.51				

The standard mesh size for B-2 is **25 millimeters**, whereas the ideal mesh size for B-2 is **50 millimeters**.

We will find a summary of the trials and errors that happened for each beam in the following table. Additionally, we will find the error table (Table 4.3) and the B-3 trials in this table. The maximum load capacity the experiment can handle is 103 kilonewtons.

The ideal and most frequent mesh size for B-3 is **25 millimeters**, which is continuous overall.

Table 4.3: Trials and errors for B-3

Trials	D-V-M	FEA	Error %	Trials	D-V-M	FEA	Error %
T 1	37-0.03-25	116.88	13.65	**T 15**	31-0.05-25	123.30	19.89
T 2	36-0.03-25	112.15	9.05	**T 16**	31-0.03-25	104.11	1.23
T 3	32-0.03-25	107.02	4.06	**T 17**	31-0.025-25	97.83	4.87
T 4	32-0.03-25	112.31	9.21	**T 18**	31-0.025-25	102.97	0.13
T 5	31-0.03-25	103.99	1.12	**T 19**	36-0.025-25	106.78	3.83
T 6	31-0.025-25	97.05	5.63	**T 20**	31-0.025-25	118.74	15.46
T 7	32-0.025-25	98.63	4.09	**T 21**	36-0.025-25	112.63	9.52
T 8	32-0.03-25	101.20	1.59	**T 22**	31-0.03-25	109.28	6.26
T 9	31-0.03-25	100.47	2.30	**T 23**	**31-0.05-25**	**128.08**	**24.54**
T 10	37-0.03-25	113.94	10.79	**T 24**	31-0.025-15	101.58	1.23
T 11	31-0.03-25	100.47	2.30	**T 25**	31-0.025-20	103.06	0.21
T 12	36-0.03-25	104.27	1.39	**T 26**	31-0.025-30	104.10	1.23
T 13	36-0.05-25	138.38	34.56	**T 27**	31-0.025-40	106.66	3.71
T 14	36-0.03-25	108.70	5.70	**T 28**	31-0.025-50	105.99	3.06

Within the scope of our investigation, the mesh analysis demonstrated a range of mesh sizes that were appropriate for experimental validation for each beam. On the other hand, after considering it, we concluded that a standard mesh size of 25 millimeters is the best option for all beams. This is because the differences in mesh sizes across beams are slight.

We ensured the exact combination applied to each of the three beams during the study. By maintaining a constant dilation angle of 31 degrees and an eccentricity of 0.1 throughout the procedure, these parameters ensured that the beams remained consistent over the length of the trial.

Eccentricity is a vital quantity to consider when assessing the behavior of structures when they are subjected to loads since it affects several parameters, including shear forces and bending moments. When evaluating the structural response and stability of components such as beams or columns, eccentricity is often considered in the context of fixed element analysis and structural modeling.

To ensure coherence, it was confirmed that the value of (Kc) was maintained consistently at 0.667 overall beams. According to the data shown in the following table (Table 4.4), the viscosity parameter showed a considerable variation when it was adjusted for the different mesh sizes that were taken into consideration.

Table 4.4: Modified Parameter

Beam No	Dilation Angle	Eccentricity	fb0/fc0	Kc	Viscosity Parameter	Mesh Size mm
B-1	31	0.1	1.16	0.667	0.04	15, 20, 25, 30, 40, and 50
B-2	31	0.1	1.16	0.667	0.05	
B-3	31	0.1	1.16	0.667	0.025	

To investigate the complex impact that viscosity has on the structural behavior of the beams, the strategic changes were implemented with great care and attention to detail. This systematic and deliberate approach allowed us to conduct our finite element analysis more effectively. Still, it also played a crucial part in enhancing our confidence in the reliability and correctness of the conclusions generated from the thorough simulation results.

Using the material parameters provided, we carefully analyzed each of the three beams, adjusting the mesh sizes methodically to understand the effect of these adjustments on the structural behavior of the beams. Using this systematic approach, we conducted a thorough study into the finite element analysis results, which enabled us to determine the mesh size most suitable for each beam. The repeated changes in mesh sizes gave vital insights into how differences in this parameter influenced the overall performance and correctness of the structural simulations. The process of iterative adjustment supplied these insights. The figure (Fig. 4.4) shows the mesh variation for the RC beam.

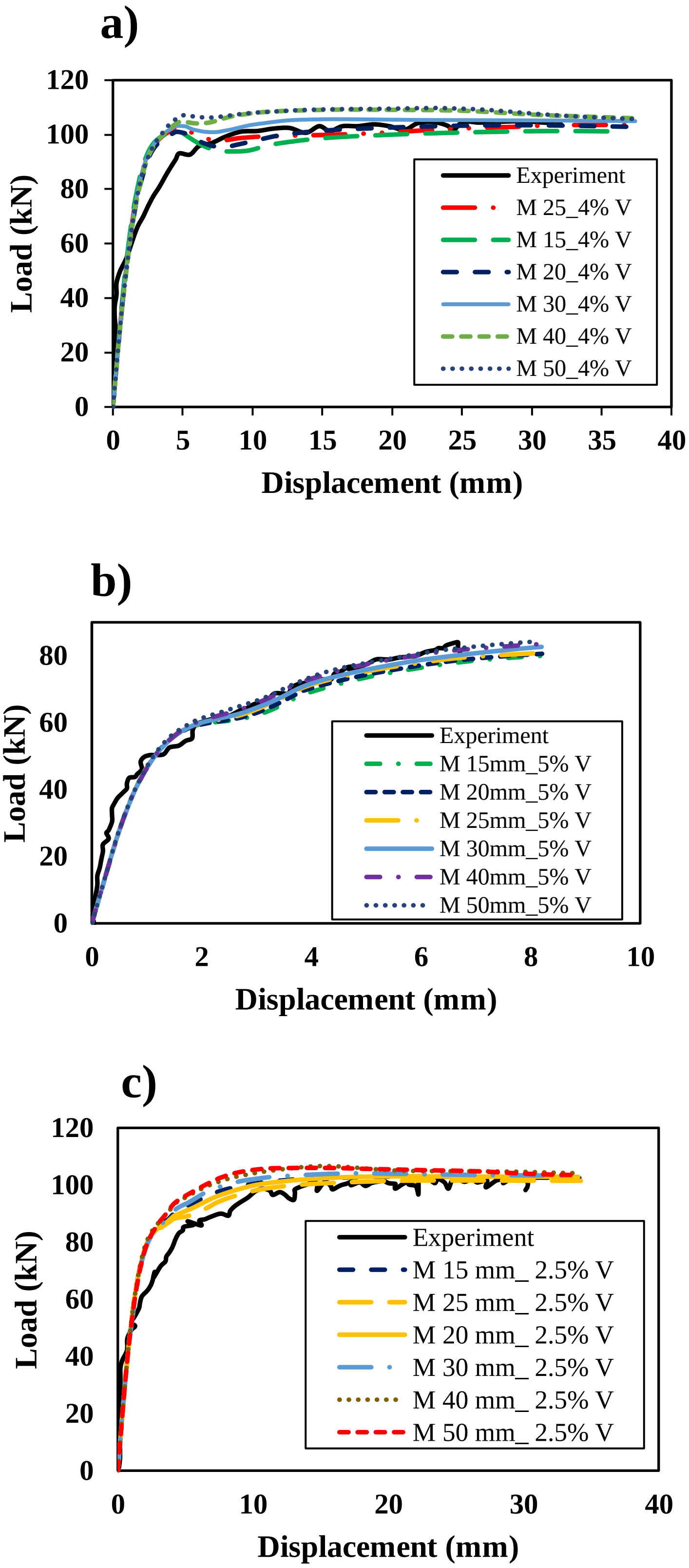

Fig. 4.4: RC beam load vs. displacement behavior at mesh variation results for a) B-1, b) B-2 and c) B-3

4.2.3.2 Synopsis

This study's primary goal is to assess the effectiveness and accuracy of various modeling approaches. This evaluation will include the change of factors such as the dilation angle, viscosity, and meshing. After comprehensively investigating each beam, the best parameters for reinforced concrete beams are determined. These parameters include a dilation angle of 31 degrees uniform across the beams and an eccentricity of 0.1. In addition, it has been determined that a consistent mesh size of 25 millimeters is the best option for all beams, which provides a systematic approach for the conduct of the research.

The beams' analysis included a table with each beam's most essential characteristics and results. This simplified presentation makes the study's findings more straightforward by providing a condensed summary of the most critical aspects and conclusions.

Table 4.5: Summary Table of Material Property

Beam No	Dilation Angle	Eccentricity	fb0/fc0	Kc	Viscosity Parameter	Mesh Size mm
B-1	31	0.1	1.16	0.667	4%	M 30mm
B-2	31	0.1	1.16	0.667	5%	M 50mm
B-3	31	0.1	1.16	0.667	2.5%	M 25mm

During our investigation, we used a variety of mesh sizes for each beam to determine the most suitable mesh size. Furthermore, it has been determined that the most appropriate option for all beams is a mesh size of 25 millimeters, which is uniform over all beams.

All the beams were compared using the usual mesh size of 25 millimeters. The illustration (Fig. 4.5: optimal and typical mesh sizes for all beams for a) B-1, b) B-2 and c) B-3) shows a significant gap between the ideal and standard mesh sizes for all beams.

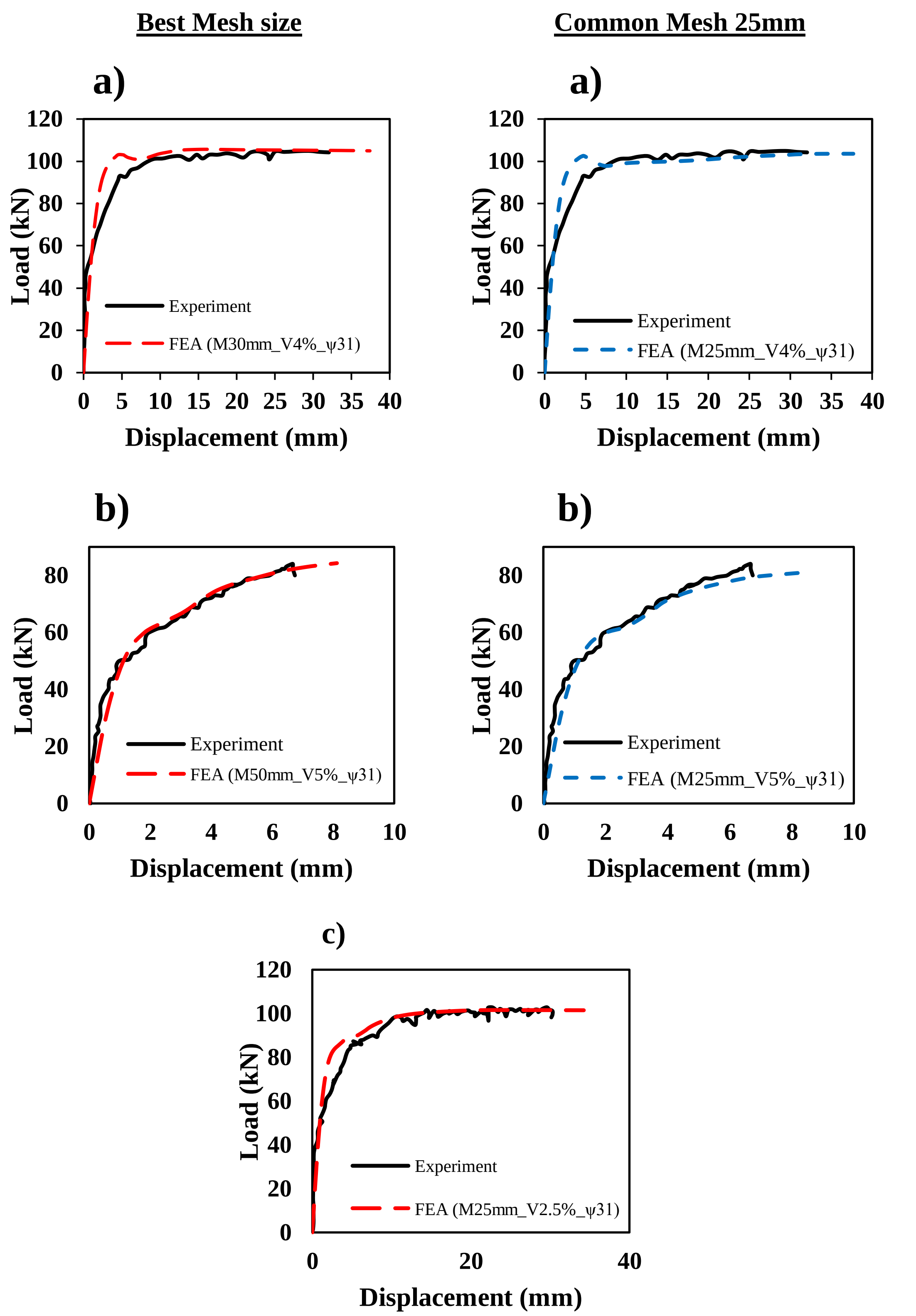

Fig. 4.5: optimal and typical mesh sizes for all beams for a) B-1, b) B-2 and c) B-3

4.3 Plot of mesh sensitivity

This section provides a systematic presentation of the mesh sensitivity control. It includes a complete figure that illustrates the changes in sensitivity across various mesh sizes. The graphic visually demonstrates the influence of variations in mesh density on the analysis findings. The graphical explanation aims to clarify the importance of choosing the appropriate mesh size and how it impacts the accuracy and reliability of the finite element analysis.

The following figures provide a comprehensive examination of the variations in mesh size for B-1, clarifying the impact of various mesh sizes on the analysis outcomes.

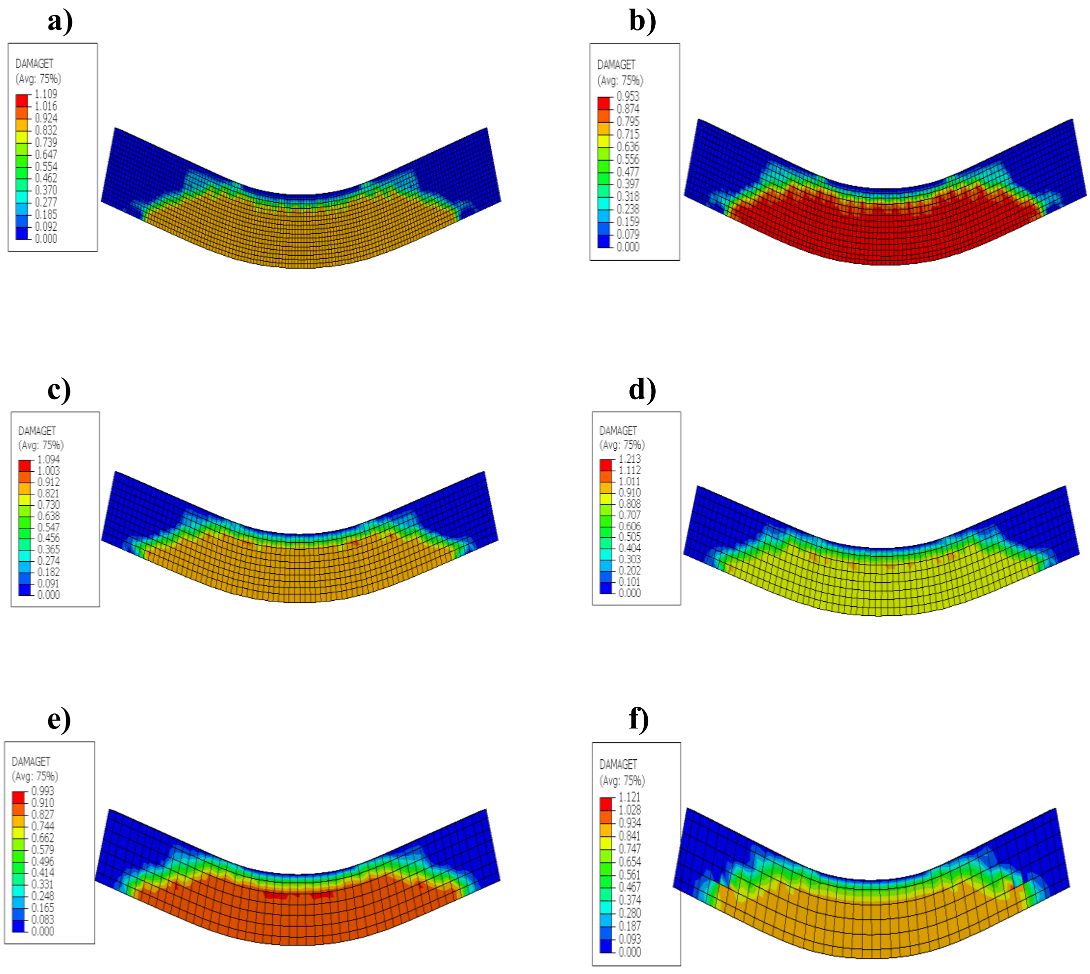

Fig. 4.6: Tension Damage for B-1 for mesh size of a) M 50mm b) M 40mm c) M 30mm d) M 25mm e) M 20mm f) M 15mm

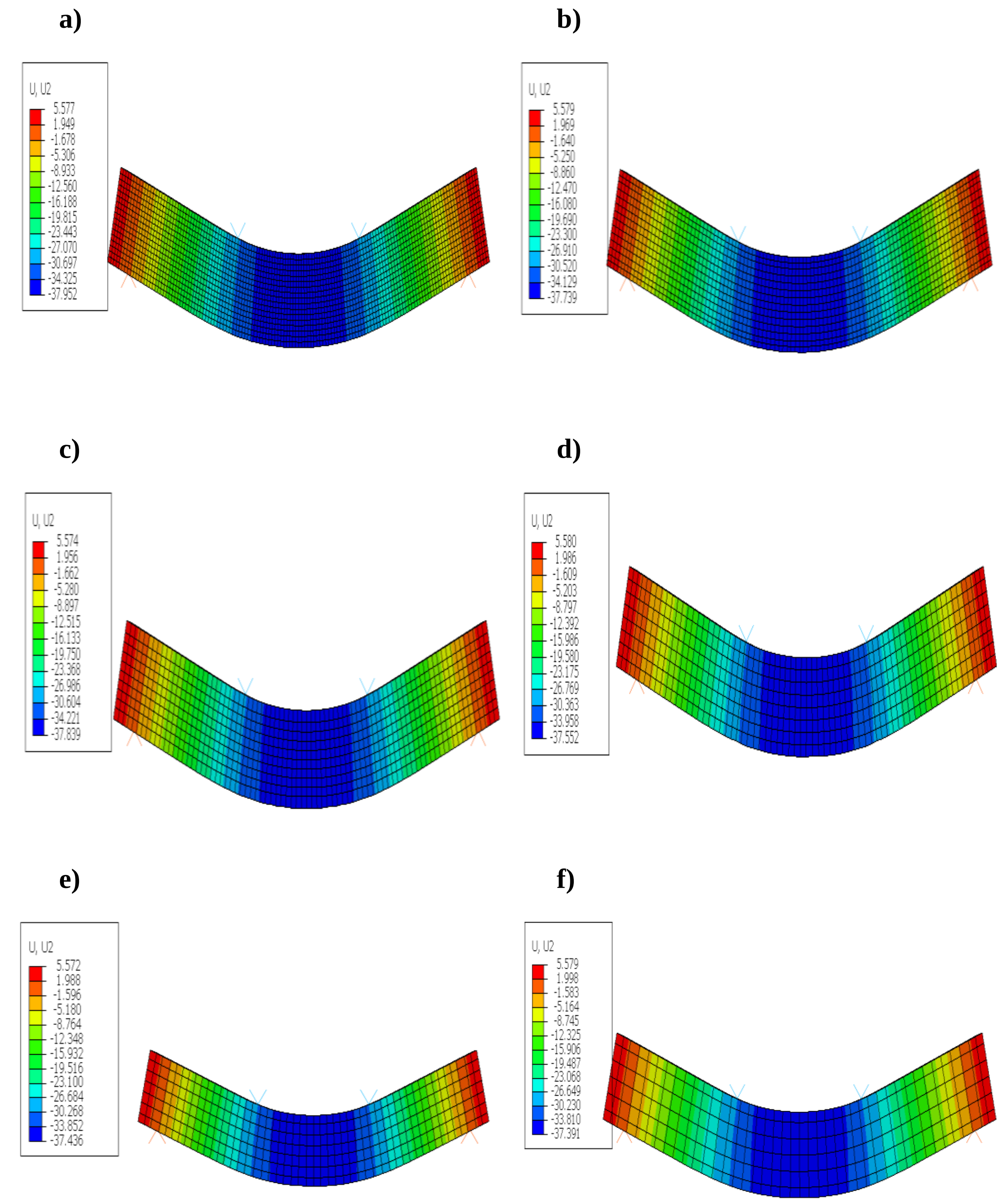

Fig. 4.7: Displacement for B-1 for mesh size of a) M 50mm b) M 40mm c) M 30mm d) M 25mm e) M 20mm f) M 15mm

The following images thoroughly examine the different mesh sizes for B-2 and show how the various mesh sizes affected the study results.

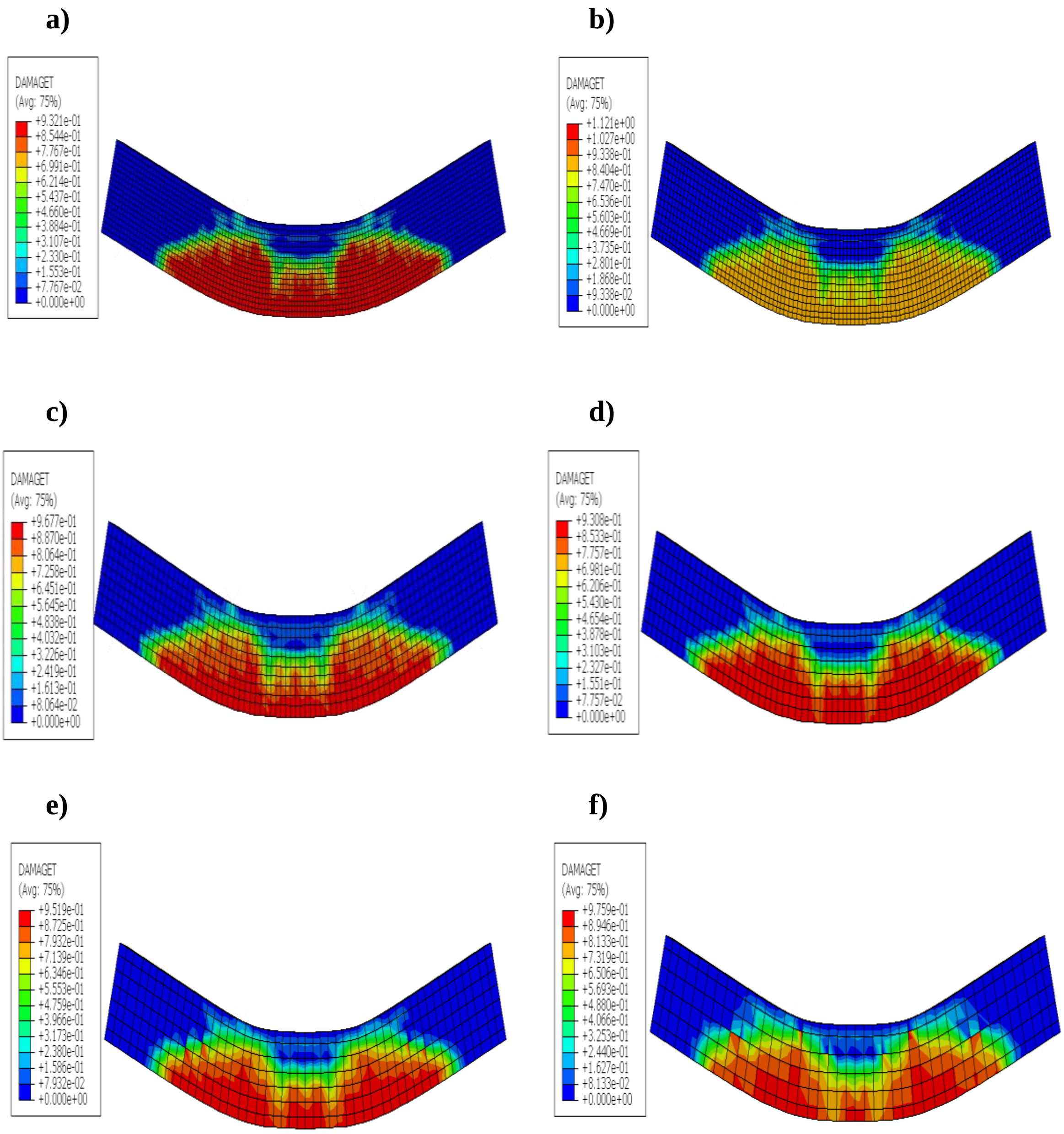

Fig. 4.8: Tension Damage for B-2 for mesh size of a) M 50mm b) M 40mm c) M 30mm d) M 25mm e) M 20mm f) M 15mm

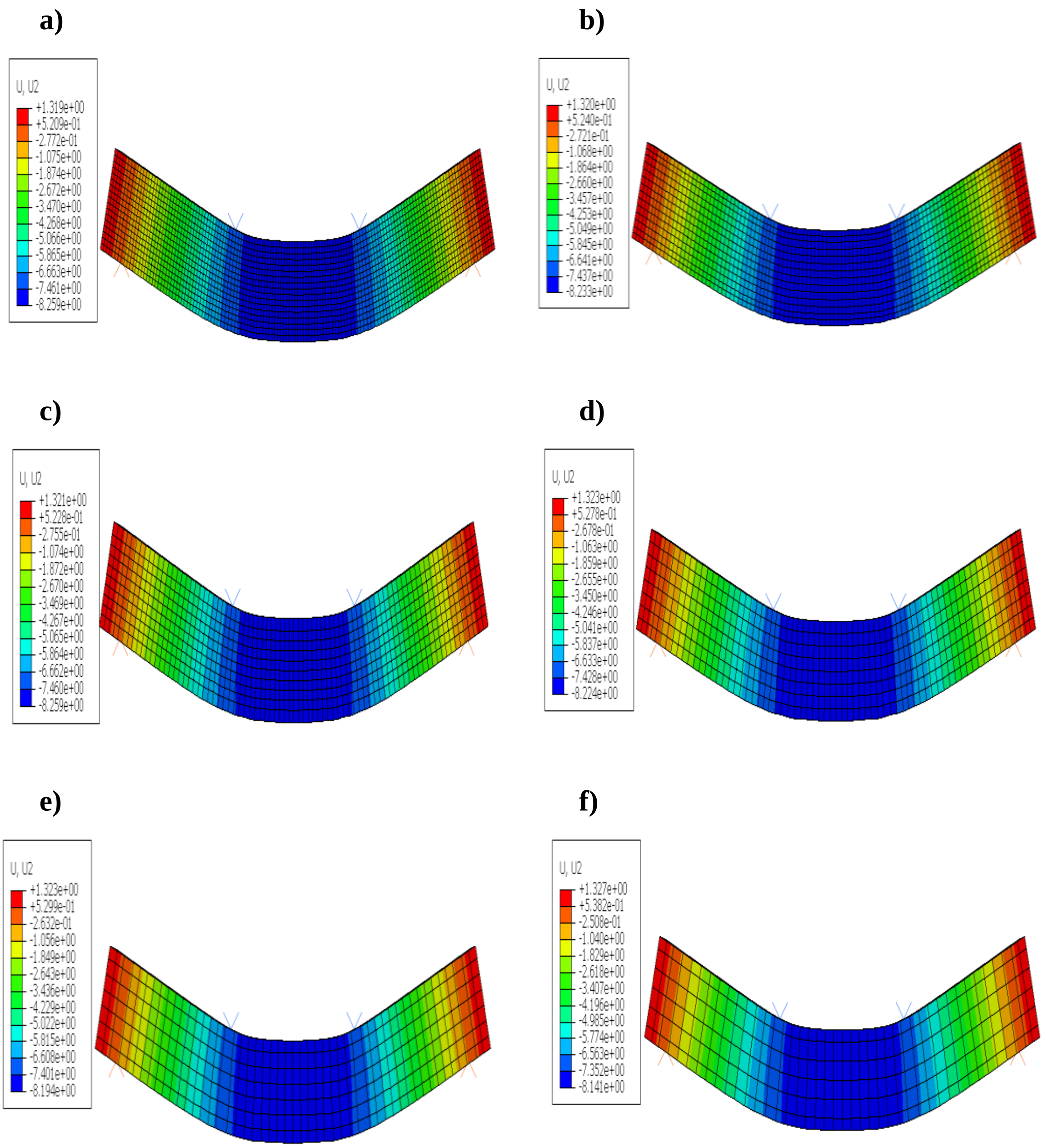

Fig. 4.9: Displacement for B-2 for mesh size of a) M 50mm b) M 40mm c) M 30mm d) M 25mm e) M 20mm f) M 15mm

The illustrations below show the different mesh sizes for B-3 and how they changed the study results.

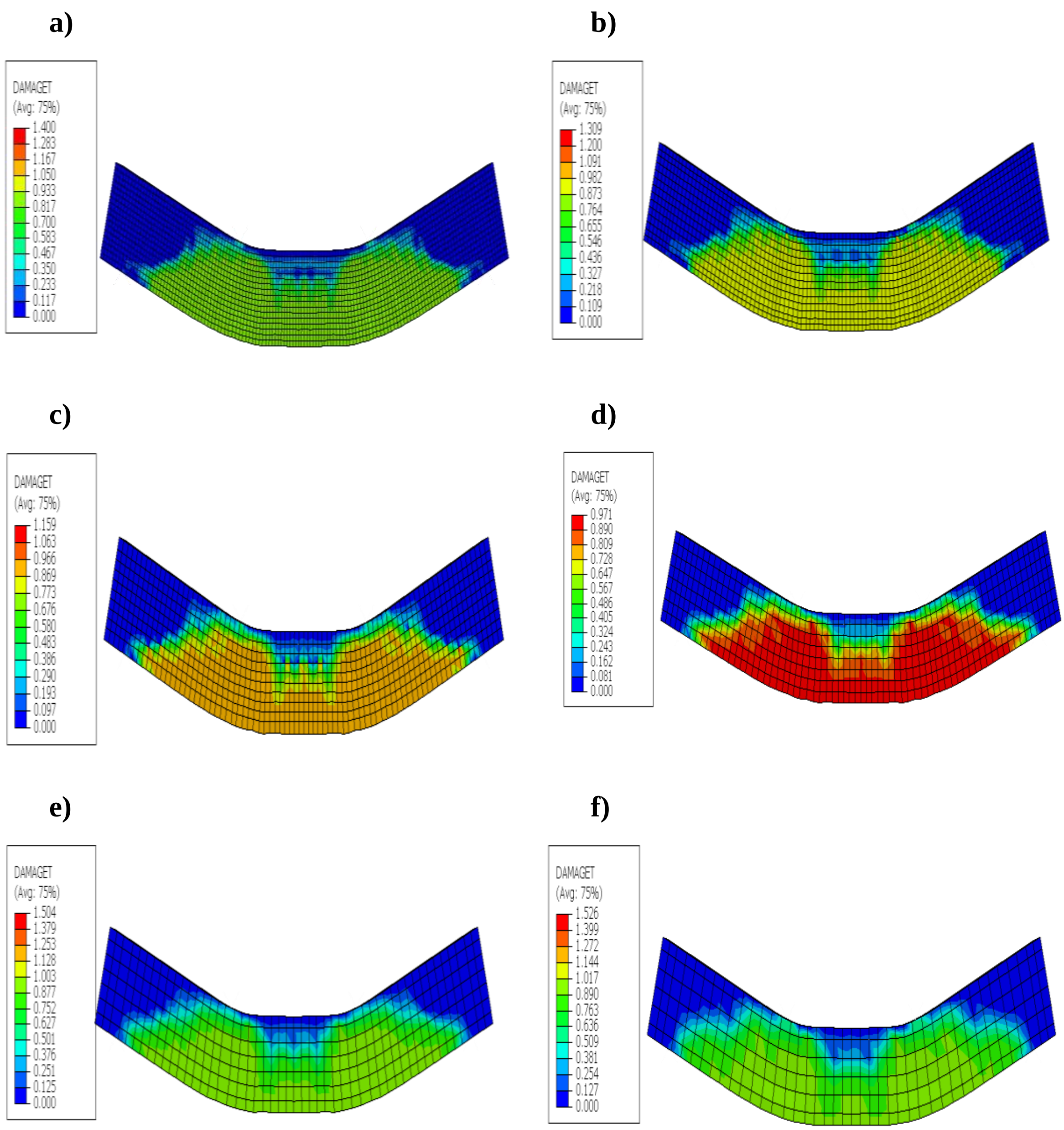

Fig. 4.10: Tension Damage for B-3 for mesh size of a) M 50mm b) M 40mm c) M 30mm d) M 25mm e) M 20mm f) M 15mm

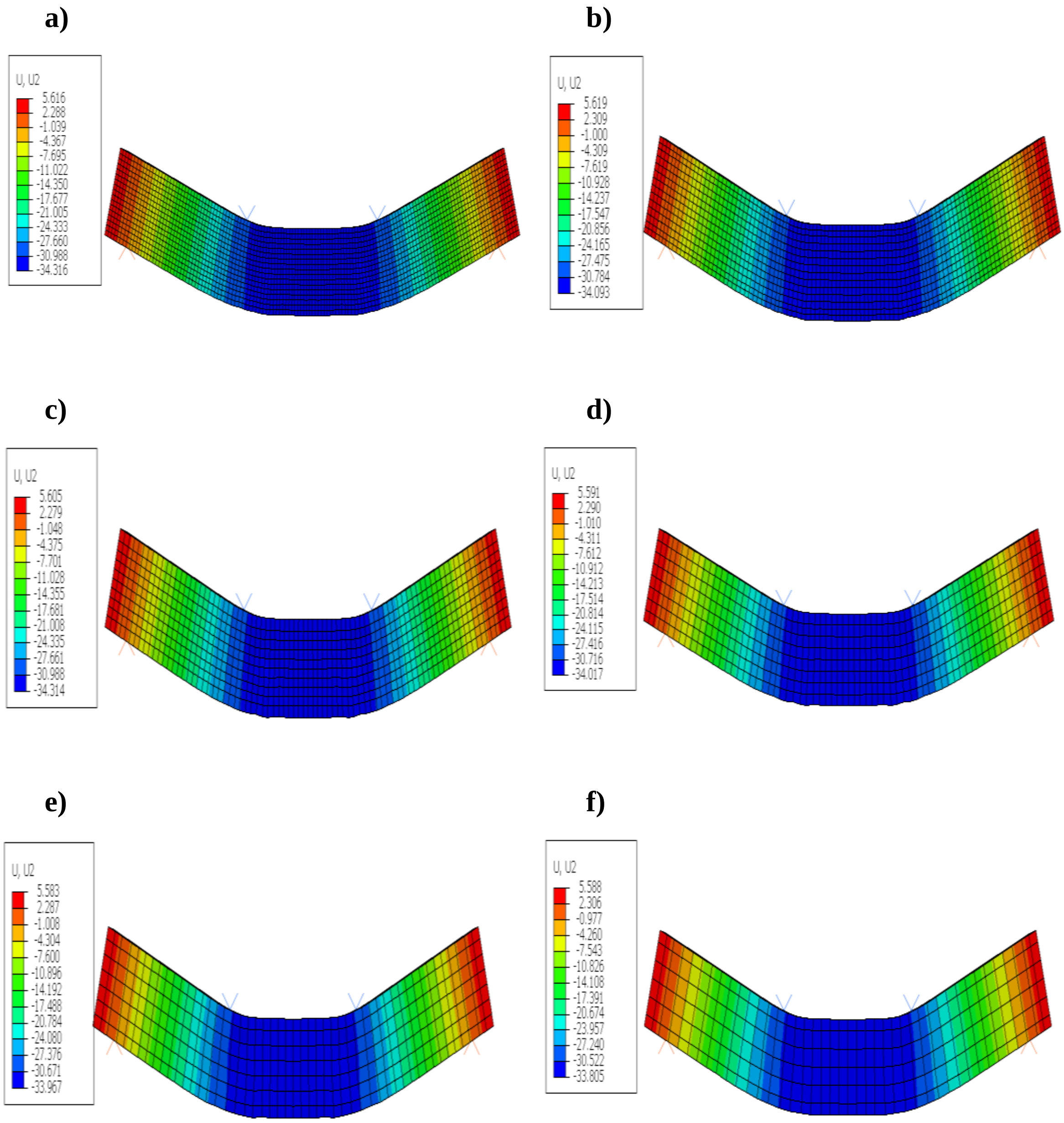

Fig. 4.11: Displacement for B-3 for mesh size of a) M 50mm b) M 40mm c) M 30mm d) M 25mm e) M 20mm f) M 15mm

4.4 Summary

The full scope of the accumulated data is presented in this chapter, which sheds light on recurring patterns identified within the simulation results. Every component is divided into sections, each focusing on different results obtained via the investigation process. The written material includes thorough pictures and graphical representations to enhance the knowledge of the findings achieved via the rigorous application of finite element analysis. This allows for a deeper understanding of the results. In addition to advancing a more comprehensive knowledge of the study's broad aims, this chapter provides essential insights into the complex behavior and performance variations of the structural components examined. It draws upon the ideas presented in the parts that came before it. A sturdy basis of analytical examination and based information explanation is provided by this all-encompassing methodology, which guarantees that the findings and observations that are produced are supported by this foundation.

CHAPTER 5
Conclusion & Recommendation

5.1 Conclusion

To summarize, the purpose of this research was to comprehensively examine the behavior of reinforced concrete beams, with a particular focus on material parameters such as dilation angle, viscosity, and mesh size. The detailed quantitative analysis, performed using ABAQUS software, effectively verified the experiment results and provided a better understanding of the complex interaction of these components—the accurate measurements of the beams allowed for a logical comparison, increasing the study's dependability. Incorporating beams with and without lap splices, diverse stirrup forms, and changes in concrete types subtly enhanced the comprehension of structural reactions. The accurate representation of the connection between concrete and steel in real life was successfully achieved, and the analytical methodology used in ABAQUS played a crucial role in modeling various situations. The study confirms the accuracy of finite element models and offers valuable insights into optimizing parameters for future assessments. After a comprehensive investigation, it was concluded that 0.04, 0.05, and 0.025 viscosity values are the most favorable for B-1, B-2, and B-3, respectively. A dilation angle of 31 exhibited successful outcomes for all beams.

The following are notable findings that resulted from this analysis:

- **i.** As a result of this comparison, a remarkable alignment and consistency were noticed between the results of the finite element simulation and the factual findings of the experiment.
- **ii.** The finite element model used specified viscosity values of 0.04, 0.05, and 0.025 for B-1, B-2, and B-3 concrete damage parameters. These values closely aligned with standard deviations and were well-validated against experimental results.

iii. The investigation demonstrated that a dilation angle of 31 degrees yielded satisfactory outcomes for all beams. Using a dilation angle range of 31 in the finite element model as a damage material parameter for concrete was reliable and in agreement with the experiment's results.

iv. All beams utilized the prevailing mesh size of 25mm. Nevertheless, separate ideal mesh sizes were determined for each beam, with a 30mm mesh size being the most appropriate for B-1 and a 50mm mesh size for B-2.

v. Through a series of analytical procedures, we were able to determine that the maximum loads for B-1 (with a concrete strength of 31.86 MPa) were 127 kN, and for B-2 (with a definite strength of 30.67 MPa) were 84 kN, and for B-3 (with a concrete strength of 32.56 MPa), were 138 kN.

vi. The results of the finite element models are close to what was observed in the experiments, especially regarding the load-deflection reaction. This means the models used to make concrete and reinforcing steel effectively capture elastic and plastic behavior.

5.2 Recommendation

In future studies using reinforced concrete beams, it is advised that similar viscosity and dilation angle values be used. This recommendation is based on the ideal parameters that have been determined. Researchers should consider the following aspects for future investigation:

I. To ensure consistency and reliable comparisons, keeping the viscosity, dilation angle, and mesh size identical for each beam in the study is strongly recommended.

II. A more detailed and accurate representation in finite element simulations may be achieved using fracture energy or displacement relationships as material characteristics instead of the conventional concrete tensile stress-strain property.

III. To properly assess the performance of reinforced concrete beams, it is recommended to conduct detailed experimental and finite element computations specially designed to account for high-strength concrete (HSC) and self-compacting concrete (SCC) qualities. This technique will provide vital insights into these specific concrete kinds' distinct attributes and efficacy, enhancing our comprehensive comprehension of their structural dynamics.

IV. It is advisable to conduct comprehensive experimental and finite element evaluations designed especially for this structural arrangement to obtain a thorough knowledge of the behavior of deep beams.

V. Diversifying lap splices in experimental and analytical studies improves investigation durability and applicability. Adding welded and mechanical splices to the lap splice can help understand structural behavior under varied situations. This method may provide helpful information about how well and often different splice designs perform on reinforced concrete beams.

VI. It is recommended to change the number of stirrups and lower the diameter of the bars in the splice zone. These alterations will cause a substantial change in how the structure fails while having a minor influence on its maximum capacity.

VII. The use of finite element approaches has the potential to significantly affect the future of design and production, facilitating the creation of creative, more efficient, and more dependable goods.

Reference

1. *Abaqus 6.14 Documentation*. (n.d.). Retrieved January 26, 2024, from http://130.149.89.49:2080/v6.14/
2. *ACI CODE-318-14: Building Code Requirements for Structural Concrete and Commentary*. (n.d.). Retrieved January 27, 2024, from https://www.concrete.org/store/productdetail.aspx?ItemID=318U14&Language=English&Units=US_Units
3. *AutoCAD 2024 Help | Autodesk*. (n.d.). Retrieved January 26, 2024, from https://help.autodesk.com/view/ACD/2024/ENU/
4. Bhuiyan, M. H., & Ahmed, S. (2022). *Post-Fire Residual Capacity of Reinforced Concrete Beam BT - Advances in Civil Engineering* (S. Arthur, M. Saitoh, & S. K. Pal (Eds.); pp. 117–126). Springer Singapore.
5. Demir, A., Ozturk, H., & Dok, G. (2016). *11-1-55-1-10-20170604*. *2*(1), 13–18.
6. Demir, A., Ozturk, H., Edip, K., Stojmanovska, M., Bogdanovic, A., & Seismology, E. (2018). *Viscosity Parameters Ofconcrete.Pdf*. *8*(3), 50–56.
7. *Eurocode 2: Design of concrete structures | Eurocodes: Building the future*. (n.d.). Retrieved January 26, 2024, from https://eurocodes.jrc.ec.europa.eu/EN-Eurocodes/eurocode-2-design-concrete-structures
8. Haavisto, J., Alho, H., & Laaksonen, A. (2023). The behavior of lap splices in reinforced concrete beams after bar yielding. *Structural Concrete*, *24*(4), 5245–5264. https://doi.org/10.1002/suco.202200501
9. Hafezolghorani, M., Hejazi, F., Vaghei, R., Jaafar, M. S. Bin, & Karimzade, K. (2017). Simplified damage plasticity model for concrete. *Structural Engineering International*, *27*(1), 68–78. https://doi.org/10.2749/101686616X1081
10. Mabrouk, R. T. S., & Mounir, A. (2018). The behavior of RC beams with tension lap splices confined with transverse reinforcement using different types of concrete under pure bending. *Alexandria Engineering Journal*, *57*(3), 1727–1740. https://doi.org/10.1016/j.aej.2017.05.001

11. Maghsoudi, A. A., & Akbarzadeh Bengar, H. (2011). The acceptable lower bound of the ductility index and serviceability state of RC continuous beams

strengthened with CFRP sheets. *Scientia Iranica*, *18*(1 A), 36–44. https://doi.org/10.1016/j.scient.2011.03.005

12. Mousa, M. I. (2015). Flexural behavior and ductility of high-strength concrete (HSC) beam with tension lap splice. *Alexandria Engineering Journal*, *54*(3), 551–563. https://doi.org/10.1016/j.aej.2015.03.032
13. Mustapha. (2023). *ep rin t n ot pe er r ed Pr ep rin t n ot pe er r ed*.
14. Najafgholipour, M. A., Dehghan, S. M., Dooshabi, A., & Niroomandi, A. (2017). Finite element analysis of reinforced concrete beam-column connections with governing joint shear failure mode. *Latin American Journal of Solids and Structures*, *14*(7), 1200–1225. https://doi.org/10.1590/1679-78253682
15. Najafgholipour, M. A., Dehghan, S. M., Khani, M., & Heidari, A. (2018). The performance of lap splices in RC beams under inelastic reversed cyclic loading. *Structures*, *15*, 279–291. https://doi.org/10.1016/j.istruc.2018.07.011
16. Nguyen, T. H., Huynh, P. D., & Le, A. T. (2020). The Load-Bearing of Concrete Beams as the Steel Reinforcements Connected by the Coupler at a Cross-Section of a Beam. *Proceedings of 2020 5th International Conference on Green Technology and Sustainable Development, GTSD 2020*, 209–213. https://doi.org/10.1109/GTSD50082.2020.9303073
17. Rohman, R. K., Kristiawan, S. A., Saifullah, H. A., & Basuki, A. (2022). Reinforcement to concrete bond strength: A comparison between normal concrete and various types of concrete. *Journal of Physics: Conference Series*, *2190*(1). https://doi.org/10.1088/1742-6596/2190/1/012028
18. Vanova, P., Dubecky, D., Weissova, M., Bartus, J., & Kvocak, V. (2023). An experimental and numerical study of twin dowel type shear connector. *Scientific Reports*, *13*(1), 1–11. https://doi.org/10.1038/s41598-023-30005-3
19. Vitanov, V. (2017). *MATERIAL MODEL OF FRP STRENGTHENED-INFORCED CONCRETE IN BIAXIAL STRESS STATE SUBJECTED TO MONO-TONIC LOADING CONDITIONS-*. *6*(1).

20. Zaioune, H., & Mezhoud, S. (2023). Numerical Analysis of Behavior of Corbels Strengthened with Carbon Fiber-Reinforced Polymer. *Iranian Journal of Science and Technology - Transactions of Civil Engineering*, *47*(4), 2149–2171. https://doi.org/10.1007/S40996-023-01062-5/METRICS

Appendix

The Tables below show all the material properties we used.

Table A. 1: Details about the concrete material for B-1

Material Property	*31.86 MPa*	**Plastic Parameter**	
		Dilation angle	31
Concrete elasticity		Eccentricity	0.1
Ec	26529 MPa	Fb_0/fc_0	1.16
Poison ratio	0.2	Kc	0.667
Concrete compressive behavior		**Concrete compressive damage**	
Stress (MPa)	Inelastic Strain	Damage C	Inelastic Strain
9.558	0	0	0
13.93875	0.000139715	0	0.000139715
23.895	0.000639715	0	0.000639715
29.86875	0.001139715	0	0.001139715
31.86	0.001639715	0	0.001639715
30.267	0.002139715	0.05	0.002139715
28.674	0.002639715	0.1	0.002639715
27.081	0.003139715	0.15	0.003139715
Concrete tensile behavior		**Concrete tensile damage**	
Stress (MPa)	Cracking Strain	Damage T	Cracking Strain
3.186	0	0	0
2.45322	3.00238E-05	0.23	3.00238E-05
1.4337	0.000360285	0.55	0.000360285
0.3186	0.000924732	0.9	0.000924732

Table A. 2: Details about the concrete material for B-2

Material Property	*30.67 MPa*	**Plastic Parameter**	
		Dilation angle	31
Concrete elasticity		Eccentricity	0.1
Ec	26029 MPa	Fb0/fc0	1.16
Poison ratio	0.2	Kc	0.667
Concrete compressive behavior		**Concrete compressive damage**	
Stress (MPa)	Inelastic Strain	Damage C	Inelastic Strain
9.201	0	0	0
13.418125	0.000146507	0	0.000146507
23.0025	0.000646507	0	0.000646507
28.753125	0.001146507	0	0.001146507
30.67	0.001646507	0	0.001646507
29.1365	0.002146507	0.05	0.002146507
27.603	0.002646507	0.1	0.002646507
26.0695	0.003146507	0.15	0.003146507
Concrete tensile behavior		**Concrete tensile damage**	
Stress (MPa)	Cracking Strain	Damage T	Cracking Strain
3.067	0	0	0
2.36159	2.94577E-05	0.23	2.94577E-05
1.38015	0.000353493	0.55	0.000353493
0.3067	0.000907298	0.9	0.000907298

Table A. 3: Details about the concrete material for B-3

Material Property	*32.56 MPa*	**Plastic Parameter**	
		Dilation angle	31
Concrete elasticity		Eccentricity	0.1
Ec	26819 MPa	Fb0/fc0	1.16
Poison ratio	0.2	Kc	0.667
Concrete compressive behavior		**Concrete compressive damage**	
Stress (MPa)	Inelastic Strain	Damage C	Inelastic Strain
9.768	0	0	0
14.245	0.000135778	0	0.000135778
24.42	0.000635778	0	0.000635778
30.525	0.001135778	0	0.001135778
32.56	0.001635778	0	0.001635778
30.932	0.002135778	0.05	0.002135778
29.304	0.002635778	0.1	0.002635778
27.676	0.003135778	0.15	0.003135778
Concrete tensile behavior		**Concrete tensile damage**	
Stress (MPa)	Cracking Strain	Damage T	Cracking Strain
3.256	0	0	0
2.50712	3.03518E-05	0.23	3.03518E-05
1.4652	0.000364222	0.55	0.000364222
0.3256	0.000934835	0.9	0.000934835

Table A. 4: Details of the Properties of the Reinforcement Material.

Yield Strength	400 MPa
Es	210 GPa
0.1 E	21000

Steel Plastic Property	
Plastic Stress	Plastic Strain
400.7619048	0
421.2	0.000950119
441.6761905	0.001899336
462.1904762	0.002847653
482.7428571	0.003795071
503.3333333	0.004741593
523.9619048	0.005687219
544.6285714	0.006631952
565.3333333	0.007575794
586.0761905	0.008518745
606.8571429	0.009460809

Table A. 5: Multiple trials for B-1 verification

B-1 (NC-L00-0T6)															
No.	**ψ**	**K**	**V**	**M**	**Es**	**Steel**	**Type**	**No.**	**ψ**	**K**	**V**	**M**	**Es**	**Steel**	**Type**
J-1	36	0.667	0.03	25	200	400/600	Linear	**J-21**	37	0.667	0.03	25	200	400/425	Linear
J-2	36	0.667	0.03	25	200	400/600	Non Linear	**J-22**	37	0.667	0.03	25	200	400/450	Linear
J-3	36	0.667	0.3	25	200	400/600	Linear	**J-23**	36	0.667	0.05	25	210	400/400	Linear
J-4	36	0.667	0.3	25	200	400/600	Non Linear	**J-24**	36	0.667	0.03	25	210	400/400	Linear
J-5	31	0.667	0.03	25	200	400/600	Non Linear	**J-25**	31	0.667	0.05	25	210	400/400	Linear
J-6	31	0.667	0.03	25	200	400/600	Linear	**J-26**	31	0.667	0.03	25	210	400/400	Linear
J-7	36	0.667	0.025	25	200	400/600	Linear	**J-27**	31	0.667	0.025	25	210	400/450	Linear
J-8	36	0.667	0.025	25	200	400/600	Non Linear	**J-28**	36	0.667	0.025	25	210	400/450	Linear
J-9	31	0.667	0.025	25	200	400/600	Linear	**J-29**	31	0.667	0.025	25	210	400/600	Linear
J-10	31	0.667	0.025	25	200	400/600	Non Linear	**J-30**	36	0.667	0.025	25	210	400/600	Linear
J-11	37	0.667	0.03	25	200	400/600	Linear	**J-31**	31	0.667	0.03	25	210	400/450	Linear
J-12	37	0.667	0.03	25	200	400/600	Non Linear	**J-32**	31	0.667	0.05	25	210	400/450	Linear
J-13	37	0.667	0.025	25	200	400/600	Linear	**J-33**	31	0.667	0.04	25	210	400/450	Linear
J-14	37	0.667	0.025	25	200	400/600	Non Linear	**J-34**	31	0.667	0.035	25	210	400/450	Linear
J-15	37	1.000	0.03	25	200	400/600	Linear	**J-35**	31	0.667	0.04	15	210	400/450	Linear
J-16	36	0.667	0.03	25	200	400/600	Linear	**J-36**	31	0.667	0.04	20	210	400/450	Linear
J-17	36	0.667	0.03	25	200	400/600	Linear	**J-37**	31	0.667	0.04	30	210	400/450	Linear
J-18	36	0.667	0.03	25	200	400/600	Linear	**J-38**	31	0.667	0.04	40	210	400/450	Linear
J-19	36	0.667	0.03	25	200	400/450	Linear	**J-39**	31	0.667	0.04	50	210	400/450	Linear
J-20	36	0.667	0.03	25	200	400/425	Linear								

Table A. 6: Multiple trials for B-2 verification

B-2 (NC-L30-0T6)															
No.	**ψ**	**K**	**V**	**M**	**Es**	**Steel**	**Type**	**No.**	**ψ**	**K**	**V**	**M**	**Es**	**Steel**	**Type**
Job-1	37	0.667	0.03	25	200	400/450	Linear	**Job-17**	36	0.667	0.05	25	210	400/400	Linear
Job-2	36	0.667	0.03	25	200	400/450	Linear	**Job-18**	36	0.667	0.03	25	210	400/400	Linear
Job-3	39	0.667	0.03	25	200	400/450	Linear	**Job-19**	31	0.667	0.05	25	210	400/400	Linear
Job-4	37	0.667	0.03	25	200	400/500	Linear	**Job-20**	31	0.667	0.03	25	210	400/400	Linear
Job-5	39	0.667	0.025	25	200	400/450	Linear	**Job-21**	31	0.667	0.025	25	210	400/450	Linear
Job-6	37	0.667	0.028	25	200	400/425	Linear	**Job-22**	36	0.667	0.025	25	210	400/450	Linear
Job-7	36	1.000	0.03	25	210	400/425	Linear	**Job-23**	31	0.667	0.025	25	210	400/600	Linear
Job-8	36	1.000	0.03	25	210	400/400	Linear	**Job-24**	36	0.667	0.025	25	210	400/600	Linear
Job-9	36	0.667	0.03	25	210	400/600	Non-Linear	**Job-25**	31	0.667	0.03	25	210	400/450	Linear
Job-10	31	0.667	0.03	25	210	400/400	Non-Linear	**Job-26**	31	0.667	0.05	25	210	400/450	Linear
Job-11	37	0.667	0.03	25	210	400/450	Non-Linear	**Job-27**	31	0.667	0.05	15	210	400/450	Linear
Job-12	31	0.667	0.03	25	220	400/400	Non-Linear	**Job-28**	31	0.667	0.05	20	210	400/450	Linear
Job-13	31	0.667	0.03	25	250	400/600	Non-Linear	**Job-29**	31	0.667	0.05	30	210	400/450	Linear
Job-14	36	0.667	0.03	25	250	400/600	Non-Linear	**Job-30**	31	0.667	0.05	40	210	400/450	Linear
Job-15	36	0.667	0.03	25	270	400/600	Non-Linear	**Job-31**	31	0.667	0.05	50	210	400/450	Linear
Job-16	36	0.667	0.03	25	280	400/600	Non-Linear								

Table A. 7: Multiple trials for B-3 verification

B-3 (NC-L30-6T6)															
No.	ψ	K	V	M	Es	Steel	Type	No.	ψ	K	V	M	Es	Steel	Type
T-1	37	0.667	0.03	25	200	400/450	Linear	T-16	31	0.667	0.03	25	210	400/400	Linear
T-2	36	0.667	0.03	25	200	400/450	Linear	T-17	31	0.667	0.025	25	210	400/400	Linear
T-3	32	0.667	0.03	25	200	400/450	Linear	T-18	31	0.667	0.025	25	210	400/450	Linear
T-4	32	0.667	0.03	25	200	400/500	Linear	T-19	36	0.667	0.025	25	210	400/450	Linear
T-5	31	0.667	0.03	25	200	400/425	Linear	T-20	31	0.667	0.025	25	210	400/600	Linear
T-6	31	0.667	0.025	25	200	400/425	Linear	T-21	36	0.667	0.025	25	210	400/600	Linear
T-7	32	0.667	0.025	25	200	400/425	Linear	T-22	31	0.667	0.03	25	210	400/450	Linear
T-8	32	0.667	0.03	25	200	400/400	Linear	T-23	31	0.667	0.05	25	210	400/450	Linear
T-9	31	0.667	0.03	25	200	400/400	Linear	T-24	31	0.667	0.025	15	210	400/450	Linear
T-10	37	0.667	0.03	25	210	400/450	Non-Linear	T-25	31	0.667	0.025	20	210	400/450	Linear
T-11	31	0.667	0.03	25	200	400/400	Non-Linear	T-26	31	0.667	0.025	30	210	400/450	Linear
T-12	36	0.667	0.03	25	200	400/400	Non-Linear	T-27	31	0.667	0.025	40	210	400/450	Linear
T-13	36	0.667	0.05	25	210	400/400	Linear	T-28	31	0.667	0.025	50	210	400/450	Linear
T-14	36	0.667	0.03	25	210	400/400	Linear								
T-15	31	0.667	0.05	25	210	400/400	Linear								